NASA/TP-2006-213672

Conceptual Design Study for an X–38 Transonic Rocket Assist Configuration

Susan J. Stachowiak, Brent R. Cobleigh, Heather A. Maliska, Masashi Mizukami,
Stephen A. Whitmore, and Timothy H. Cox
NASA Dryden Flight Research Center
Edwards, California

March 2006

NASA STI Program ... in Profile

Since its founding, NASA has been dedicated to the advancement of aeronautics and space science. The NASA scientific and technical information (STI) program plays a key part in helping NASA maintain this important role.

The NASA STI program is operated under the auspices of the Agency Chief Information Officer. It collects, organizes, provides for archiving, and disseminates NASA's STI. The NASA STI program provides access to the NASA Aeronautics and Space Database and its public interface, the NASA Technical Report Server, thus providing one of the largest collections of aeronautical and space science STI in the world. Results are published in both non-NASA channels and by NASA in the NASA STI Report Series, which includes the following report types:

- TECHNICAL PUBLICATION. Reports of completed research or a major significant phase of research that present the results of NASA programs and include extensive data or theoretical analysis. Includes compilations of significant scientific and technical data and information deemed to be of continuing reference value. NASA counterpart of peer-reviewed formal professional papers but has less stringent limitations on manuscript length and extent of graphic presentations.

- TECHNICAL MEMORANDUM. Scientific and technical findings that are preliminary or of specialized interest, e.g., quick release reports, working papers, and bibliographies that contain minimal annotation. Does not contain extensive analysis.

- CONTRACTOR REPORT. Scientific and technical findings by NASA-sponsored contractors and grantees.

- CONFERENCE PUBLICATION. Collected papers from scientific and technical conferences, symposia, seminars, or other meetings sponsored or co-sponsored by NASA.

- SPECIAL PUBLICATION. Scientific, technical, or historical information from NASA programs, projects, and missions, often concerned with subjects having substantial public interest.

- TECHNICAL TRANSLATION. English-language translations of foreign scientific and technical material pertinent to NASA's mission.

Specialized services also include creating custom thesauri, building customized databases, and organizing and publishing research results.

For more information about the NASA STI program, see the following:

- Access the NASA STI program home page at *http://www.sti.nasa.gov.*

- E-mail your question via the Internet to help@sti.nasa.gov.

- Fax your question to the NASA STI Help Desk at (301) 621-0134.

- Phone the NASA STI Help Desk at (301) 621-0390.

- Write to:
  NASA STI Help Desk
  NASA Center for AeroSpace Information
  7121 Standard Drive
  Hanover, MD 21076-1320

NASA/TP-2006-213672

Conceptual Design Study for an X–38 Transonic Rocket Assist Configuration

Susan J. Stachowiak, Brent R. Cobleigh, Heather A. Maliska, Masashi Mizukami,
Stephen A. Whitmore, and Timothy H. Cox
NASA Dryden Flight Research Center
Edwards, California

National Aeronautics and
Space Administration

Dryden Flight Research Center
Edwards, California 93523-0273

March 2006

Cover art: Photo courtesy of Brent R. Cobleigh.

NOTICE

Use of trade names or names of manufacturers in this document does not constitute an official endorsement of such products or manufacturers, either expressed or implied, by the National Aeronautics and Space Administration.

Available from the following:

NASA Center for AeroSpace Information
7121 Standard Drive
Hanover, MD 21076-1320
(301) 621-0390

National Technical Information Service
5285 Port Royal Road
Springfield, VA 22161-2171
(703) 605-6000

CONTENTS

ABSTRACT 1

NOMENCLATURE 1

INTRODUCTION 2

EARLY TRADE STUDIES 4
- Transonic Boost Vehicle Selection 4
  - Vehicle 131R 4
  - Vehicle 132 4
  - Vehicle 133 4
  - Vehicle Recommendation 5
- Propulsion System Type 5
  - Liquid Rocket 5
  - Solid Rocket 5
  - Propulsion Recommendation 6
- Propulsion Integration 6
  - Internal 6
  - Aft 6
  - Top 6
  - Bottom 7
  - Side 7
  - Rocket Integration Recommendation 7

PROPULSION 7

WEIGHT AND BALANCE 10
- X-38 Transonic Rocket Assist Mass Properties 11
- Ballast Management System 13
- Moments of Inertia 14

SIMULATION STUDIES 14
- Simulation Setup 15
- Rocket Model 15
- Constraints 16
- Configuration and Trajectory Development 16
- Programmed Test Inputs 18
- Motor Performance Dispersion Effects 18
- Simulation Conclusions 20

STRUCTURAL DESIGN 20
Attachment Structures 20
Forward External Attachment Structure 21
Aft External Attachment Structure 22
Rocket Jettison Configuration 22
Preliminary Loads 22
Design Loads 23
Vehicle Clearances 23
Ground Clearance 23
Access Panels 24
Structural Conclusions 24

THERMAL CONSIDERATIONS 24
Cold Soak of the Rocket Motors 24
Cold-Soak Analysis.....24
Rocket Plume Heating 25

GROUND TESTS 26
Primary Ground Tests.....26
Wind Tunnel Test 26
Rocket Pressure–Bending Test 27
Captive-Carry Test 27
Ignition and Flight Termination System Tests 27
Ballast Dump–Jettison Test.....27
Hook Loads Test 27
Secondary Ground Tests.....27
Rocket Jettison Test 27
Ground Vibration Test.....27
Attachment Hardware Static Loads Test.....28

LAUNCH–RANGE OPERATIONS 28

CONCLUSION 28

REFERENCES 31

FIGURES 32

ABSTRACT

The X-38 Transonic Rocket Assist feasibility and conceptual design study examined the possibility of obtaining transonic flight data for the X-38 program by boosting an existing X-38 airframe into the transonic flight regime. The objective of the study was to develop a conceptual design to collect X-38 transonic aerodynamic flight data. This report summarizes the work performed by the conceptual design team in developing a proposed XTRA configuration. Initial study phases focused on selecting the appropriate vehicle to use for the transonic flight-test program, selecting the most appropriate propulsion system, and integrating the propulsion system with the X-38 vehicle. The final design featured two 10,000-lb thrust rocket motors, externally mounted on the sides of an X-38 flight-test vehicle. A detailed structural loads analysis of this configuration was performed and structure required for rocket attachment and jettison systems was designed. A ballast management system was developed to control changes in center of gravity caused by rocket burn and jettison. Simulation studies were performed to optimize the XTRA trajectory for maximum data collection potential and to identify any vehicle controllability issues. Simulation studies with this configuration show the potential for obtaining flight-test data at Mach numbers of up to 1.5.

NOMENCLATURE

A	aft attachment point
b	wingspan
BBMk1	Black Brant model Mk1
$\bar{c}$	mean aerodynamic chord
CG	center of gravity
CPIA	Chemical Propulsion Information Agency
CRV	crew return vehicle
C_L	lift coefficient
DFRC	Dryden Flight Research Center
F	forward attachment point
FS	fuselage station
FTS	flight termination system
g	acceleration due to gravity, 9.8 m/s^2
$\dot{h}$	altitude rate
I	moment of inertia, slug/ft^2
Isp	specific impulse
JSC	Johnson Space Center
L/D	length-to-diameter ratio

LOC	loss of control
NASA	National Aeronautics and Space Administration
OML	outer mold line
PTI	programmed test input
$\bar{q}$	dynamic pressure
Q	heat transfer rate, Btu/s
S	wing area
Tinit	initial temperature
TA_WALL	adiabatic wall temperature
TBULK	predicted bulk mass temperature
TTS	thrust termination system
TT2	stagnation temperature
TWALL	predicted external wall temperature
T_∞	ambient temperature
V	vehicle, followed by designation
x	vehicle x-axis
X-CG	x-axis center of gravity
XTRA	X-38 transonic rocket assist
y	vehicle y-axis
Y-CG	y-axis center of gravity
z	vehicle z-axis
Z-CG	z-axis center of gravity
α	angle of attack
β	angle of sideslip
ε	rocket pitch installation angle
λ	rocket yaw installation angle
σ	standard deviation

INTRODUCTION

The X-38 program consisted of five prototype vehicles designed to serve as technology demonstrators for the emergency crew return vehicle (CRV) for the International Space Station. The CRV and the X-38 prototypes were wingless, lifting-body-type vehicles based on the X-24A (Martin Aircraft Company, Baltimore, Maryland) that was flight-tested at the NASA Dryden Flight Research Center, Edwards, California (DFRC) in the late 1960s and early 1970s (ref. 1). These

vehicles operated autonomously and used a steerable parachute called a parafoil for final descent and landing. Manual control of the vehicle was possible during the parafoil phase of flight. The X-38 vehicles were unmanned.

Four of the five X-38 vehicles were designed for atmospheric flight-testing only. As these vehicles had no propulsion systems, they were carried to altitude under the wing of a B-52 airplane (The Boeing Company, Chicago, Illinois) and released, as shown in figure 1(a). The other X-38 vehicle, designated vehicle 201 (V201), was designed for space flight-testing. This vehicle was planned to be released from the Space Shuttle payload bay and then reenter the earth's atmosphere, covering a Mach number range of Mach 25.0 through subsonic on its maiden flight.

Historically, wind tunnels have had difficulties in accurately predicting the transonic aerodynamics on lifting bodies. Thus, transonic flight-test data were desired to minimize the aerodynamic uncertainties on the X-38 V201 flight-test program. However, because of the velocity limitations of the B-52 airplane while carrying an X-38 vehicle, and the lack of a propulsion system on the X-38 vehicle, the project had no method for obtaining flight data above Mach 0.80 prior to the first flight of V201.

At the request of the NASA Johnson Space Center, Houston, Texas (JSC), the NASA DFRC initiated a feasibility and conceptual design study to examine the possibility of attaching rockets to one of the atmospheric X-38 vehicles. These rockets would be ignited after vehicle release from the B-52 airplane to boost the X-38 vehicle into the transonic flight regime to collect the desired data for the V201 program.

Initial phases of the study focused on selecting the appropriate vehicle to use for the transonic flight-test program, selecting the most appropriate propulsion system, and integrating the selected propulsion system with the X-38 vehicle. Three of the X-38 atmospheric flight-test vehicles (V131R, V132, and V133) were candidates for vehicle selection. Both solid and liquid propulsion systems were initially considered and numerous rocket mounting positions for the solid rocket motors were examined.

Once the vehicle and propulsion system were selected, a preliminary structural analysis was performed and the hardware required for rocket attachment and jettison was designed. A thermal analysis was performed to determine the effects of cold-soak on the solid rockets. The effect of rocket plume heating on the base of the X-38 vehicle was examined. A ballast control system was developed to control the movement of the vehicle center of gravity (CG) during rocket burn and jettison segments of flight. Simulation studies were performed to determine the best placement of the rockets on the X-38 vehicle, to identify any controllability issues, and to estimate the expected amount of data collection. Effects of motor performance dispersions on trajectory and controllability were studied. Launch and range concerns were also addressed.

This report presents the important findings related to this study. These findings show the potential for obtaining flight-test data at Mach numbers up to 1.5.

EARLY TRADE STUDIES

Several early trade studies were conducted to narrow the candidate vehicle designs. These studies involved selecting the appropriate vehicle to use for the transonic flight test program, selecting the most appropriate propulsion system, and integrating the selected propulsion system with the X-38 vehicle.

Transonic Boost Vehicle Selection

The development of the Space Station CRV has resulted in the construction of numerous flight-test platforms. The candidate platforms for use in the transonic flight-test program included three of the X-38 vehicles designed for atmospheric flight-testing: V131R, V132, and V133. Earlier lifting bodies were not considered for use because of the instrumentation, control and guidance, and landing systems that would need to be developed; and extensive outer mold line (OML) modifications that would be necessary.

Vehicle 131R

Vehicle 131R is fully equipped with instrumentation and flight control systems that include control laws similar to V201, and a programmed test input (PTI) system to perform aerodynamic extraction maneuvers at transonic Mach numbers. In addition, V131R is an 80-percent scale OML match to the expected V201 OML. Since the transonic experiments would be conducted at the end of the V131R flight-test program, a catastrophic loss of the aircraft would not jeopardize other tests. Since V131R was in active flight test, the transition to the transonic boost configuration would have been easier than bringing an aircraft out of storage.

There were a few drawbacks to using V131R. The use of single-string flight control systems decreases the reliability of the tests and complicates range planning; the required rocket modification would also have disrupted the X-38 flight-test program.

Vehicle 132

Vehicle 132 has an internal configuration nearly identical to that of V131R, including the flight control systems, chute systems, and instrumentation. It also had the potential benefit of being available for modification without impacting the flight-testing of V131R. The major drawback, however, is that the OML change that was completed on V131R would have to be repeated for V132. This would have been a significant increase in cost, but potentially could have eliminated some of the downtime between the V131R baseline flight-testing and the XTRA configuration flight-testing.

Vehicle 133

The third option was to modify V133 to the transonic boost configuration. Vehicle 133 was designed with the correct full-size OML, PTI system, instrumentation system, and an upgraded triple-redundant flight control system. However, it had several drawbacks that made it an undesirable

choice for the transonic boost experiments. First, V133 was tasked to man-rate the parafoil system. This important task made loss of the vehicle unacceptable. Second, V133 was overweight. At 25,000 lb the vehicle was too heavy to allow modification to carry a propulsion system using the planned B-52 airplane launch system. Third, the flight-testing of V133 was scheduled to be conducted too close to the flight of V201 to have an impact on the flight control system of V201.

Vehicle Recommendation

Vehicles 131R and 132 were both acceptable for the transonic boost mission. Vehicle 131R has the correct OML but would have had to halt its flight-test program for the required configuration modification. Vehicle 132 was available for reconfiguration, but would have required an expensive modification to match the V201 OML. Because of cost considerations, V131R was chosen as the recommended vehicle for the XTRA flight program.

Propulsion System Type

Early simulations showed the need for a large total impulse (>1,000,000 lb-sec) in order to reach the desired transonic flight conditions. Both solid and liquid rockets were considered for the XTRA propulsion system. The benefits and problems of each of these propulsion systems are described in the following three subsections.

Liquid Rocket

Liquid rocket engines may be shut down at any time, and many can be throttled. Storage of the liquid propellant within the X-38 vehicle would also allow a smaller, lower-drag, external rocket profile (as compared with an externally mounted solid rocket). Locating the fuel in the forward fuselage would help to balance the aft-mounted rocket engines. Liquid rockets, however, have several drawbacks. The biggest drawback is the design or modification of the propellant feed system and the operational complexities involved with liquid propellants. Also, in the existing configuration there is not adequate space inside the vehicle for propellant tankage. Selecting a liquid rocket would result in higher design and testing costs as compared with a solid rocket, and would increase schedule uncertainty.

Solid Rocket

Numerous solid rocket motors are available off the shelf. This eliminates the need for most of the development, modification, and testing of the selected propellant system. Many of the appropriate solid rockets have long, successful launch histories. In addition, for a small number of flights, solid rockets are clearly less expensive to procure and integrate into the X-38 vehicle. Solid motors, however, cannot be throttled or normally shut down. Therefore, thrust termination for flight termination is a consideration. Also, if more than one motor is used, asymmetrical thrust can result from dispersions or single motor failures. Motor dispersions presented the largest obstacles to the XTRA design, as will be shown in the “Simulation Studies” section.

Propulsion Recommendation

Solid rocket motors are clearly the best choice for this limited flight-test application. They are available off the shelf, are relatively inexpensive, and present less difficulty for integration into the X-38 vehicle. Additionally, solid rocket motors present less potential for development problems that could lead to significant schedule slips.

Propulsion Integration

Numerous propulsion system mounting locations were considered for the XTRA configuration. The benefits and pitfalls of each of the mounting locations are described in the following six subsections.

Internal

Several of the lifting body programs used internal rocket propulsion to achieve supersonic Mach numbers. Internal integration offers many benefits. Because the rocket would be aligned with the vehicle CG, no large moments would be generated. In addition, the aerodynamic shape of the X-38 vehicle would be unaltered; therefore, no jettison of the propulsion system would be required. The major problem with internal integration is that the aft internal structure of the X-38 vehicle is filled with the parafoil system. Removal of this system would significantly degrade the recovery probability of the X-38 vehicle. Use of the backup chute as the primary chute could be considered, however, this method may result in significant damage after each flight. Base and internal heating of the X-38 vehicle could also be problematic with an internal mounting. Removal of the parafoil would also eliminate any control of the trajectory after chute deployment, since the backup chute has no steering capability.

Aft

Upper-stage rocket motors exist which could be integrated into the base region of the X-38 vehicle and jettisoned after burnout. As will be shown below, all aft-mounted rockets require significant forward ballasting in order to maintain the vehicle CG within limits. Unfortunately, this ballast results in a CG that is too far forward after rocket jettison. Aft integration of the rocket would also change the base flowfield, which could significantly lower the pitch control effectiveness of the body flaps. In the event that an aft-mounted jettison failed, the parafoil deployment would be blocked.

Top

Upper mounting of the propulsion system has numerous drawbacks. First, the rockets would have to allow for the B-52 airplane pylon attachment. Second, failure of the jettison would prevent parafoil deployment. Third, the rocket jettison away from the X-38 vehicle would require significant energy to overcome gravitational forces, and would risk collision with the vertical fins. Fourth, top mounting would produce a pitch-down moment that would fight the pull-up maneuver that is required to intercept the desired V201 trajectory.

Bottom

Lower mounting of the rocket has several benefits. These include availability of strong attach points, ease of rocket jettison, clearance from the parafoil, and minimal distance between the rocket and vehicle CG. The aft end of the rocket would have to be located far away from the surface of the X-38 in order to clear the body flaps, and far enough aft to prevent rocket plume impingement on the X-38 vehicle. One drawback of this installation is that the rocket would disrupt the lower surface flowfield and diminish the longitudinal control effectiveness of the X-38 vehicle. Failure of the jettison system would also prevent the use of the landing skids. In addition, the offset from the vehicle vertical CG would require a substantially canted nozzle to direct the thrust line through the CG. Canting the nozzle could require an expensive development program.

Side

Dividing the thrust between two side-mounted rockets offers several benefits. First, the rockets can be adjusted in vertical position and longitudinal incidence angle in order to optimize the pitching moment contribution of the rocket. Second, variation of the incidence angle of the rocket with respect to the X-38 vehicle allocates part of the rocket thrust to the vertical axis. This vertical thrust aids in the pull-out maneuver, which will be described below. Third, the rockets can be mounted such that the nozzle is cantilevered aft of the X-38 vehicle base, reducing heating concerns. Fourth, failure of the rocket jettison will not jeopardize the successful landing of the X-38 vehicle. The biggest risk of the side-mounted rocket involves the possibility of asymmetrical thrust resulting from single engine failure or performance dispersions between the two rockets. Failure of one of the side-mounted rockets will result in a loss of control. Rocket dispersions effects will be discussed in the "Simulation Studies" section below.

Rocket Integration Recommendation

The side-mounted rockets offer the best solution for the XTRA configuration. The side mounting allows more flexible optimization of the rocket forces and moments and allows a reasonable jettison prior to collecting aerodynamic data. Part of this optimization includes the redirection of the thrust line to increase the X-38 vehicle vertical component of thrust during the required pull-up maneuver. Side mounting offers no difficulties for captive-carry or parafoil deployment, and the X-38 vehicle could be safely landed after failure of the jettison system.

PROPULSION

With the selection of a solid rocket motor as the XTRA propulsion system an effort to size and select an appropriate off-the-shelf motor was conducted. The performance dispersions and reliability were also examined.

General requirements for the rocket motor were determined by the configuration and mission concept. The motor had to have a high length-to-diameter (L/D) ratio to accommodate side attachment and to better distribute the motor mass. Preliminary motor performance requirements were assessed using an in-house-developed two-dimensional trajectory code. On the order of

1,000,000 lbf-sec of total impulse was needed to reach Mach 1.4. The total impulse determined the approximate motor mass. For a typical vacuum specific impulse of 260 s and fuel fraction of 0.8, the required motors weigh about 4800 lb total, or 2400 lb each for two (ref. 2). With these guidelines, a search for the best-suited solid motor was conducted.

The major classes of available mid-size solid rocket motors are now described. Launch vehicle upper-stage motors have high performance, but have a low L/D ratio, to accommodate integration with a launch vehicle and payload. Military tactical motors are of the desired shape, but they are usually classified, which substantially complicates the project and mission logistics. In addition, many are high-thrust, short-burn-time boost stages, which are not the desired characteristics for this application, as discussed in the "Simulation Studies" section below. Sounding rocket motors appear to be the most promising category. These have high L/D ratios and extended burn times, and are openly available (ref. 3). The screening and selection of motors was accomplished using a simple two-dimensional trajectory code, as well as some early six-degree-of-freedom (6-DOF) nonlinear simulation work.

The selected motor was the Black Brant Mk1 (model 26KS20000 Mk1) rocket motor, shown in figure 2 and produced by Bristol Aerospace of Winnipeg, Manitoba, Canada. The rocket motor specifications are given in table 1. The Black Brant Mk1 was the only motor found to meet all criteria for performance, weight and balance, shape, availability, and unclassified status. The propellant is an aluminized hydroxyl-terminated polybutadiene (HTPB). The grain is a two-slotted finocyl, which provides an approximately constant thrust profile.

Table 1. Black Brant Mk1 rocket motor specifications.

Item	Specification
Motor mass	2,633 lbm
Propellant mass	2,211 lbm
Post-fire mass	400 lbm
Vacuum total impulse at 70 ºF	586,400 lbf-sec
Typical thrust	20,000 lb
Burn time	29 s
Throat area	12.3 in^2
Exit area	135.9 in^2
Operating–storage temperature range	–10 ºF to approximately +125 ºF

The Mk1 variant has improved performance over the baseline motor, found to be useful in achieving mission objectives. This variant has the same hardware and systems as the baseline motor, but has upgraded propellants and liner.

The nozzle is fixed and gimbaled. Structural hard points are at the front end for payload and nosecone attachment, and at the aft end for fin and nozzle attachment. In a typical sounding rocket stage application, thrust loads are taken in the nose of the motor casing. The rocket casing bulges slightly while the motor is burning, which precludes an attachment that rigidly clamps around the motor casing.

Jettisoning the motors prior to burnout is not recommended, because the motors continue to produce thousands of pounds of thrust, while the nearly-spent motors weigh only about 400 lb. As a result, the separated motors will have tremendous acceleration, and without fins are unstable in flight. To prevent possible collision with the X-38 vehicle and for range safety considerations, separation should take place after burnout.

The performance dispersions for the baseline motor are given in table 2. These data were obtained from numerous flights, and portions of the data were reconstructed from trajectory data.

Table 2. Rocket motor nominal performance dispersions, three-sigma.

Item	Three-sigma
Total impulse	1.3 percent
Ignition delay	0.1 s
Burn time	2.5 s
Thrust misalignment	0.2 deg
Off-axis thrust	0.23 in

During 6-DOF simulations, it was found that burn-time dispersions caused substantial asymmetric thrust during the burnout transient, leading to vehicle loss of control. The other dispersions were found to be survivable. Dispersion effects on flight will be discussed in greater detail in the “Simulation Studies” section below.

An effort was undertaken by the manufacturer to reduce or more tightly characterize the burn-time dispersion. First, effects caused by factors not relevant for two motors flown simultaneously on the same vehicle, such as ambient temperature and pressure, were removed. Second, production techniques could be tailored to reduce performance differences between motors. The analytical model predicted that burn-time dispersions could be reduced from 2.5 s to less than 0.86 s for the three-sigma case. To determine the achievable burn-time dispersion reduction with greater confidence, more detailed analyses and testing would be required.

Other means to deal with asymmetric thrust were also considered, but were not part of this conceptual design. Thrust could be terminated early in the burnout transient, to eliminate the unpredictable thrust decay. The motor is available with a flight termination feature, which blows opposing holes of about 12 by 3 inches near the front of the casing. Combustion should cease rapidly as chamber pressure is lost, thereby terminating thrust. However, this would have been a

destructive event, intended for range safety uses. Also, the extent of flames venting out of the holes and possibly damaging the vehicles are not well understood. Finally, shock loads caused by this event are not well characterized. Therefore, the motor flight termination feature is not considered a viable option for nominal end-of-boost thrust termination. An alternative thrust termination method proposed by the manufacturer is the use of a linear explosive charge to sever the nozzle assembly. This is expected to be a cleaner event, with any flames venting out the aft end of the motor, and the motor casing structure remaining mostly intact. But it would require a fairly substantial effort to design and test a new thrust termination system (TTS). Another approach would be to develop a canted nozzle to vector the thrust and reduce undesired asymmetric forces, but this too would be a nontrivial development effort.

The expected reliability and flight qualification of the motor in this application were assessed. The baseline Black Brant motor has an extensive history of over 500 flights with an excellent success rate of 98.5 percent. Test data with the Mk1 variant is limited. The only differences from the baseline motor, however, are the propellant and liner composition, with which the manufacturer has extensive experience in a different motor. Therefore, the reliability is anticipated to be comparable to the baseline motor. Assuming that a major malfunction of either motor would be catastrophic for the X-38 vehicle, the expected motor success rate is about 97.0 percent [$(98.5/100)^2$ x 100]. Decrease in motor reliability, if any, caused by the unconventional XTRA application, was difficult to quantify.

The lower operating and storage temperature limit of the motor is –10 ºF, whereas the standard temperature at an altitude of approximately 40,000 ft during captive-carry flight is –70 ºF. Cold-soak of the motor to below allowable limits is a concern, and is analyzed in the "Thermal Considerations" section below. Ignition at altitude is not expected to be a problem, because the motor can be used in sounding rocket upper-stage applications.

In summary, the Black Brant Mk1 motor was deemed to have the necessary performance and qualifications for the XTRA mission. The burn-time dispersion reductions need to be determined with greater confidence by more detailed analyses and testing. To further develop the concept, the near-field rocket plume should be characterized to better evaluate acoustic and thermal loads on the airframe. The effect of boost trajectory *g* loads on the motor structure should also be considered.

WEIGHT AND BALANCE

Early two-dimensional simulations of the X-38 transonic boost experiment identified the approximate rocket impulse that was required to attain the desired flight conditions. Once the impulse was established, the weight of the rocket followed from solid rocket chemistry. Although the weight of the selected rocket motor pair (approximately 5200 lb) was not too heavy for the B-52 airplane pylon or for the X-38 structure, the placement of the weight will require an active weight and balance system. The XTRA mass properties including the active weight and balance system are discussed in the following three subsections.

X–38 Transonic Rocket Assist Mass Properties

The placement of the rockets (such that the nozzle is aft of the vehicle base) is dictated by the requirement to avoid plume impingement onto the X-38 structure. The aft installation of the rockets results in an unacceptable change in the mass distribution, requiring forward ballast to maintain the CG forward of the aft limit. To minimize the amount of ballast required, a long rocket was preferred over a stubby rocket. The longer rocket results in a more forward CG, while still maintaining an aft nozzle position.

The modified X-38 simulation, discussed below, was used to define the allowable aft CG limit of the aircraft. The stability boundary appeared to be at an x-axis center of gravity (X-CG) position near fuselage station 166 (FS166). The baseline X-CG is at approximately FS160. A 2-in. margin was applied to the aft stability boundary to define the allowable aft X-CG limit at FS164. To keep the CG forward of the FS164 boundary, some of the existing ballast was moved from aft to forward locations and additional ballast was added to the forward fuselage. Table 3 lists the weight changes and X-CG locations of the XTRA configuration components. In addition to the rocket and ballast weights, the rocket attachment hardware is listed. The attachment hardware is split between the portion that is permanently internal to the X-38 vehicle and the external structure that will be jettisoned with the spent rockets.

Table 3. Weight and x-axis center of gravity of the X-38 transonic rocket assist configuration components.

Item	Weight, lb	X-CG, in.
Baseline 131R	17,459.0	160.3
Removed ballast:		
Parafoil bay floor	–392.3	215.8
Parafoil bay starboard floor	–52.0	219.0
Back-up chute tube bottom	–336.8	154.8
Added fixed items:		
Rocket attach forward left	50.0	186.0
Rocket attach forward right	50.0	186.0
Rocket attach aft left	10.0	316.0
Rocket attach aft right	10.0	316.0
Ballast — rocket balance	1,505.0	45.0
Added jettisonable items:		
Rocket attach forward left	112.5	186.0
Rocket attach forward right	112.5	186.0
Rocket attach aft left	27.5	316.0
Rocket attach aft right	27.5	316.0
Rocket left	2,633.0	210.7
Rocket right	2,633.0	210.7
Total (launch)	23,849.0	164.0

The total XTRA configuration weight is estimated to be approximately 23,850 lb, which is over 1,000 lb lighter than the maximum weight limit.

The X-38 vehicle has additional X-CG restrictions when the parafoil is deployed. The forward X-CG limit with the parafoil deployed is FS144.9. Table 4 presents the weight and CG position following the rocket burnout and jettison. Unfortunately, the CG after parafoil deployment is 4.9 in. forward of the allowable limit. Thus, the requirements of having aft rockets for heating concerns and forward ballast to manage the CG for controllability have resulted in an out-of-specification forward CG following parafoil deployment. A similar CG problem exists for any of the potential aft-mounted rocket installation locations. This constraint forces the use of a ballast management system.

Table 4. Weight and x-axis center of gravity of the X-38 transonic rocket assist configuration, post-parafoil deployment.

Item	Weight, lb	X-CG, in.
XTRA launch configuration	23,849.0	164.0
Parafoil assembly (7500 ft^2)	–1,470.0	216.3
Parafoil drogue chute	–354.0	269.1
Parafoil foil drogue chute retainer assembly	–12.0	269.1
Parafoil drogue chute sling assembly	–128.8	222.8
Parafoil pilot chute, sabot, et cetera	–14.2	277.0
Parafoil cover	–98.0	222.0
Rocket attach forward left	–112.5	186.0
Rocket attach forward right	–112.5	186.0
Rocket attach aft left	–27.5	316.0
Rocket attach aft right	–27.5	316.0
Rocket left	–2,633.0	210.7
Rocket right	–2,633.0	210.7
Total (parafoil deployed)	16,226.0	140.0

Ballast Management System

The only practical solution for managing the CG involves utilizing jettisonable or movable ballast. Three potential ballast control methods were considered. The first method involves jettison of approximately 800 lb of ballast from FS45. This jettison would take place after the rocket jettison and before the parafoil deployment. The best timing would be shortly after rocket jettison so that the rocket casings and ballast would fall in the same general range area and the vehicle weight would be reduced as early as possible. The ballast jettison feature would require some type of actuator, pneumatic, or mortar system for release; this would add an additional failure mode to the vehicle operation. Additionally, some of the worst-case dispersion runs (discussed below) show that large bank angles could result at the end of the rocket burns. Release of a large weight while at high bank angles could result in damage to the X-38 vehicle.

The second ballast management system involves the use of an 800-lb water tank (2.35-ft cube) at FS45. After rocket ignition, the water could be continuously released through the bottom of the fuselage. This would eliminate the range safety hazard of releasing an 800-lb slab of metal. The water can be drained with redundant pumps or pressure-fed with compressed gas bottles. Alternately, a large enough hole might allow gravity feed of the water out of the tank. Between rocket ignition and drogue chute deployment, 180 s are available during which to complete the water jettison. To prevent freezing at high altitude, antifreeze would need to be added to the water, or electrical heating elements could be wrapped around the water system hardware. Installation

of the water tank would require the electronics that are located in the forward avionics bay to be relocated. If the tank cannot be designed to fit at FS45, additional tank volume would be required to move the tank aft.

The third and last ballast management method uses a water tank at FS45 containing somewhat more than half (approximately 500 lb) the ballast water of the previous method. Instead of dumping this water overboard, however, the water is pumped to (an) aft-mounted tank(s) through one-way valves. The water could be moved using redundant pumps or some type of pressure system driven by pressurized bottles. As a result, this system would have more failure points than the two systems previously described. The lower water weight compared with the previous method will not result in a lower initial vehicle weight, since the difference would have to be made up with alternate ballast. The 500 lb of water would require an approximately 2-ft cube tank.

The water-dump method is the preferred ballast management system for the XTRA configuration, if sufficient volume is available to house the required tank at the forward fuselage station. The backup recommendation is for a jettisonable ballast, released simultaneously with or shortly after the rocket jettison.

Moments of Inertia

Adding a rocket system to the X-38 vehicle would cause large weight increases in the fore, aft, and outboard regions of the vehicle that have greatly increased the moments of inertia. Table 5 compares the moments of inertia of the standard and rocket-equipped X-38 vehicle. The simulation has shown that these increases do not adversely affect the handling of the vehicle. Once the rockets and ballast have been jettisoned, the inertias are close to the original configuration. All ballast components were treated as point masses. Attachment hardware moments of inertia were calculated from eight separate point masses. The rocket inertias were calculated using equal mass distributed cylinders plus components because of the rocket offsets from the reference axes.

Table 5. Comparison of baseline and modified X-38 moments of inertia.

Inertia, slug/ft^2	Baseline X-38, V131R	XTRA
Ix	3,484	10,258
Iy	23,284	33,324
Iz	23,950	40,302

SIMULATION STUDIES

Extensive modifications were made to the NASA DFRC X-38 simulation in order to develop and study the XTRA configuration. The primary objective of the simulation studies was to determine the best rocket configuration for boosting the X-38 V131R to transonic Mach numbers without exceeding the dynamic pressure limit of the vehicle. The vehicle was considered to be

"on-condition" when matching the Mach number and angle of attack of the V201 re-entry trajectory. The goal for maximum Mach number was 1.4 to 1.6, with the vehicle on-condition for data collection throughout the transonic region. Simulation studies sought to maximize the on-condition Mach number and data collection time. Interception of the V201 altitude trajectory was considered desirable, but of secondary importance. The suitability of the X-38 vehicle control laws for the XTRA mission was evaluated in the simulation. An overview of the modifications and results of these studies is discussed in the following seven subsections.

Simulation Setup

Vehicle 131R weight, CG, and inertias were used for simulation studies. Table 6 shows a summary of V131R properties. The aerodynamic database for V201 was used along with the appropriate V131R reference values. Later studies used a preliminary version of the V201 Multi-Application Control Honeywell (MACH) (Honeywell, Morristown, New Jersey) control laws, edited for use with V131R. Effects caused by aerodynamic deviations, turbulence, or winds were not considered in these studies. Launches were performed with the simulation's B-52 airplane aerodynamic interaction effects disabled.

Table 6. Predicted Vehicle 131R baseline properties.

Item	Value
Weight	17,459 lb
S	162 ft^2
b	23 ft
$\bar{c}$	23 ft
X-CG	160.25 in
Y-CG	–0.05 in
Z-CG	28.35 in
Ixx	3,484 slug/ft^2
Iyy	23,197 slug/ft^2
Izz	23,863 slug/ft^2
Ixz	–19 slug/ft^2
Ixy	210 slug/ft^2
Iyz	–39 slug/ft^2

Rocket Model

For the purposes of these studies, the X-38 piloted simulation was updated with the ability to model V131R with two rockets attached. The thrust for each rocket was modeled at the nozzle exit plane, and included altitude corrections and thrust variations with time. Rocket ignition time

(nominally 5 s after launch) was user-settable. Rocket CG positions and rocket installation angles (pitch and yaw) were set by the user. Figures 3 and 4 show the pitch and yaw installation angles as they were defined in the simulation. Static weight, CG, and inertia changes caused by the solid rockets, rocket attachment hardware, and ballast addition and movement were accounted for in the simulation. Dynamic mass property changes caused by fuel burn, ballast dump, rocket CG travel, and rocket jettison were also modeled. Estimated changes in the vehicle lift and drag caused by the rockets (based on published data of flow over a cylinder) were accounted for before rocket jettison. Interference effects were not considered. Rocket jettison was assumed to be instantaneous and removed both rockets and all external attachment hardware; internal attachment hardware remained with the vehicle. The simulation modeled each rocket separately and had the ability to perform several types of asymmetric burns. The simulation also had the capability to model both the plate and water-drop types of ballast jettison that were considered.

Constraints

The dynamic pressure limit of the vehicle was the dominating constraint in determining the rocket configuration and flight profile. The dynamic pressure limit was implemented in the simulation as a function of normal load, as shown in figure 5. The vehicle dynamic pressure limit for 1-*g* flight was 500 psf and decreased linearly to 340 psf at the vehicle normal load limit of 3 *g*. There is some uncertainty as to whether or not these dynamic pressure limits would be acceptable to the project, which currently uses a 300 psf dynamic pressure limit during flight-testing. However, no configuration using the rocket motors could be found that achieved the desired Mach numbers while keeping dynamic pressure below the current project limit. Most trajectory runs showed dynamic pressure nearing the limits defined in figure 5. The vehicle normal load limit of 3 *g* did not prove to be problematic, as typical simulation runs showed a maximum of less than 2 *g*.

Rocket position was set to ensure vehicle clearance from the rocket plume and to satisfy vehicle weight and balance requirements, as has been described above. Both the pitch and yaw rocket installation angles were limited by physical constraints, such as bulkhead locations and access panels, and to allow adequate clearance between the rockets and the ground and the B-52 airplane.

Configuration and Trajectory Development

To reduce the potential for exceeding dynamic pressure limits during rocket burn, the vehicle needs to transition to a climb before excessive Mach number is built up. Once sufficient dynamic pressure margin was available, a pushover was performed to turn the flight path downward and build Mach number. After rocket burnout, this downward flight path helped to reduce the Mach number bleed-off rate, thereby increasing the data collection time.

To find the configuration that would get the vehicle as close as possible to this ideal trajectory, a series of trade studies were performed. These trade studies varied available parameters one at a time and in combination to show their effects on overall performance. Parameters varied included thrust values, rocket burn time, rocket position on the X-38 vehicle, rocket installation angles, launch conditions, and angle-of-attack profile.

As a baseline, the rockets were mounted with a zero-degree pitch installation angle with respect to the X-38 vehicle x-axis at the vehicle z-axis CG (Z-CG) position. Angle-of-attack command was held constant at 18 deg.

In this configuration the vehicle had difficulty transitioning to climb, as shown in figure 6. The desired Mach numbers were obtained, but the dynamic pressure was beyond maximum allowable values, as can be seen in figure 7. In addition, the vehicle began to climb near rocket burnout and continued to climb throughout data collection maneuvers in the transonic region. This climb caused a rapid bleed-off of Mach number, resulting in a short time on test condition, as shown in figure 8.

While having no effect on the ability of the vehicle to transition to climb, launching the vehicle at higher altitudes had a positive effect on keeping the dynamic pressure within limits. Therefore, a launch altitude of 46,000 ft (2,000 ft lower than the maximum achieved in captive-carry flight) was selected as the launch altitude for all future rocket studies.

Studies also showed that lower-thrust, longer-burning rockets allow the vehicle to reach higher Mach numbers without exceeding the above-defined dynamic pressure limits of the vehicle. Using these types of rockets would also allow for a high-altitude interception of the V201 re-entry trajectory. However, the desired burn times were not available in solid rockets with the long, slender casings that are required for weight and balance.

Of the remaining options, the addition of a pitch installation angle (ε) had the most positive effect on helping the vehicle transition to climb, as shown in figure 9. When the pitch angle is positive (nose up), a portion of the rocket thrust is used to augment lift of the X-38 vehicle. Rocket Z-CG position was chosen to approximately cancel out the pitching moments caused by the rocket angle (see figure 10). For these runs, the angle-of-attack command profile was held constant at 18 deg. Higher pitch installation angles may be desirable for initiating climb, but physical constraints such as structural attachment and ground clearance limited this angle to less than 12 deg.

In addition to lowering the maximum dynamic pressure, increased pitch installation angle also lowered the maximum Mach number achieved. To recover the lost Mach number, the angle-of-attack command flight profile was changed to push-over to a low angle of attack once the climb had been initiated.

The maximum dynamic pressure remained approximately the same as with the zero-angle configuration but it now occurred at a lower normal acceleration (Nz) value, shifting it to within vehicle limits, as shown in figure 11. Using the push-over technique, maximum Mach numbers increased with increased pitch installation angle. However, because of the short burn time of the rocket motors, sufficient time was not available to reestablish angle of attack before rocket jettison. Since some Mach number was lost while the vehicle returned to an 18-deg angle of attack, on-condition Mach numbers and data collection times were slightly decreased by installing the rockets with a nose-up pitch angle.

Programmed Test Inputs

A set of PTIs consisting of rudder, aileron, and elevator doublets respectively was initiated during a typical trajectory to illustrate data collection for determining aerodynamic coefficients. Figure 12 shows a sample trajectory illustrating the use of PTIs. These PTIs were designed based on experience with V132 free-flight 002. The magnitudes and width of the doublets were set to give sufficient excitation of the aircraft. Separation between the yaw and aileron doublet was designed to provide information on the unforced response of the vehicle. Each set of rudder, aileron, and elevator doublets was designed to fit within a 10-s window. The philosophy behind the PTI design was to start the first window after rocket burnout when the vehicle was close to the desired test condition of a 16-deg angle of attack and then repeat the window as many times as possible until the Mach number became lower than 0.8. A representative set of PTIs showed the possibility of performing several sets of doublets including two rudder and aileron doublets and one elevator doublet at or above Mach 1.0. The actual number of PTIs achieved depends on the final trajectory.

Motor Performance Dispersion Effects

With one rocket mounted on each side of the vehicle, motor performance dispersions became a major concern. The simulation showed that the failure of one rocket to ignite would result in a loss of control. Even if both rockets ignite, slight differences between the rockets had the potential to negatively impact the ability of the vehicle to maintain control during rocket burn. The following motor performance dispersion simulation studies address the potential impact of these differences on both vehicle survivability and mission success.

Three types of motor performance dispersions (suggested by the manufacturer) were considered in simulation studies: ignition time, thrust magnitude, and burn time. For each dispersion type, simulation runs were made with one-, two- and three-sigma dispersion values provided by the manufacturer. The vehicle was considered to have not survived if it departed controlled flight, inverted at any point during the run (even if recovering after rocket burnout), or if dynamic pressure was outside of limits. The X-38 flight software has a loss of control (LOC) flag that is set if predefined pitch, roll or yaw rates are exceeded. The LOC rate limits used during the XTRA study were the same as the limits used during the V131R flight test: 30 deg/sec in pitch, 50 deg/s in roll and 20 deg/s in yaw. During dispersion studies, LOC rates were exceeded on several of the simulation runs; however, in most of these cases, the vehicle was able to recover on its own with minimal impact on the remainder of the flight. This suggests that LOC rates may be set too low for these tests. Rocket burn segments of the XTRA flights may require that values for LOC rates be increased or that the LOC flag be disabled.

Differences in thrust values between the two rockets had extremely small effects on the vehicle. Loss of control was not a problem even under maximum tested dispersions. Three-sigma dispersions resulted in a small roll-off around both rocket ignition and burnout times, as can be seen in figure 13. No LOC rates were exceeded. There was little or no effect on the maximum values of Mach number, dynamic pressure, or data collection time.

For ignition time dispersions all cases were survivable. No LOC rates were exceeded for one-sigma thrust dispersions. The current LOC rates were exceeded in roll for two-sigma and three-sigma dispersion magnitudes. Figure 14 shows the three-sigma dispersion magnitudes. The yaw rate for three-sigma dispersions approached the LOC limit, as shown in figure 15. Ignition time dispersions cause the vehicle to become a bit "wobbly," with oscillations developing in both the roll and yaw axes. For all cases, the vehicle returns to wings-level within 15 s, and there is minimal impact on data collection.

Burn-time motor performance dispersions had the most negative impact on vehicle survivability. The vehicle could not withstand a two-sigma dispersion as currently defined by the manufacturer. However, as discussed in the "Propulsion" section above, burn-time dispersion values can be reduced by some amount by neglecting factors that are not applicable to the XTRA mission. With this in mind, an analysis was conducted to estimate a dispersion magnitude that may be more applicable to the XTRA configuration. Based on this analysis, simulation studies assumed 0.86 s as the three-sigma burn-time motor performance dispersion value. Later analysis shows that this dispersion magnitude may be too optimistic.

Maximum burn-time motor performance dispersions caused large roll rates around rocket burnout. These roll rates typically exceeded the LOC rates, and often caused the vehicle to perform 360-deg rolls or depart controlled flight. Simulation studies were performed to find the maximum tolerable burn-time dispersion values for a variety of rocket configurations. Simulation studies also focused on changes to the rocket installation that could help the vehicle survive the estimated three-sigma dispersion of 0.86 s.

Simulation studies showed the pitch installation angle to be a key factor for vehicle survivability under a burn-time motor performance dispersion. When the pitch installation angle is nonzero, a component of the rocket thrust acts in the z-axis. With rockets mounted over six feet from the vehicle centerline, these forces have a large moment arm and thus create very large rolling moments. When there is a difference in thrust between the two rockets, these rolling moments do not cancel each other, and large roll rates may result. Although survivable, large roll disturbances are not acceptable.

To demonstrate this, a series of simulation studies were performed. These studies varied the pitch installation angle and observed vehicle reaction to the three-sigma second motor performance dispersion. For higher pitch installation angles, the vehicle performed 360-deg rolls at rocket burnout. As the pitch installation angle was lowered, the roll rates and bank angles caused by the motor performance dispersion decreased. This can be seen in figure 16. Although still showing a significant bank angle at rocket burnout, the vehicle was able to recover with minimal effect to data collection for the 2.5-deg rocket installation angle. With an 11-deg pitch installation angle, the vehicle was unable to maintain control under the same dispersion (figure 17).

To find the maximum tolerable dispersions, simulation runs were performed with installation angles ranging from 0 deg to 10 deg. For each angle, the burn-time dispersion was increased until the vehicle inverted at burnout. Results showed that maximum survivable burn-time dispersion

decreases with increasing pitch installation angles (see figure 18).

Results of the motor performance dispersion studies suggest that the pitch installation angle should be kept as low as possible to avoid excessive rolling moments at rocket burnout. However, as discussed above, some positive installation angle is needed to keep the vehicle within dynamic pressure limits. Therefore, studies were performed to assess the effectiveness of a reduced moment arm at minimizing rolling moments under burn-time dispersions. For these studies, a yaw installation angle as defined in figure 4 was introduced. The pitch installation angle was held constant at 11 deg, and the vehicle reaction to the three-sigma dispersion was observed for several yaw installation angles. Simulations having toe-out installation of the rockets resulted in decreased roll rates and bank angles at rocket burnout, as shown in figure 19. This toe-out has the added benefit of moving the rocket forebody away from the X-38 vehicle to provide larger clearance to the side access panels.

Simulation Conclusions

The X-38 transonic boost design is capable of obtaining aerodynamic data at Mach numbers up to Mach 1.5. Data collection time varied with flight profile and rocket installation angles, but was generally in the 20 s to 60 s range. Simulation of the side-mounted solid rocket XTRA configuration revealed two primary difficulties: keeping the dynamic pressure below current limits, and surviving a large burn-time dispersion. The dynamic pressure limitation was maintained by installing the rockets with a nose-up attitude that directs a portion of the thrust to augment the vehicle lift. This resulted in a transition to a climb at a lower Mach number. The burn-time dispersion effects were relieved by canting the rockets outboard or reducing the rocket pitch installation angle, or both. However, the burn-time dispersions defined by the manufacturer were too large for the X-38 vehicle regardless of rocket installation. Several manufacturing methods were identified to reduce dispersion magnitudes. If the burn-time dispersions remain too large to control, the thrust could be terminated near burnout using the TTS described above.

STRUCTURAL DESIGN

The attachment of two rockets to the side of the X-38 V131R raised several structural concerns. These concerns include thrust loads, rocket attachment, rocket jettison, and dynamic loads.

The following ten subsections will address these issues by presenting the conceptual design and preliminary analysis results.

Attachment Structures

The design of the attachment structures addresses several issues including attachment location on the vehicle, attachment location on the rocket, and rocket motor case bending and bulging. With the above issues considered, a conceptual design of the attachment structure was developed. The designs and concepts presented below are based on information provided by the rocket manufacturer, information provided by the vehicle manufacturer, and consultation from the structures group at NASA JSC.

The forward and aft vehicle rocket attachment locations require sturdy bulkheads or longerons to react the aerodynamic, acceleration, and thrust loads. As shown in figure 20 as STA 193, the forward attachment location at FS193 is accessible to tie into. The bulkhead at station FS193 also serves as the load path for the hook attachment on the B-52 airplane. The aft attachment location is shown to tie into the aft bulkhead of the vehicle. Internal systems such as landing gear actuators, rudder actuators, and access doors must be avoided.

The decision to attach to the rockets at FS193 (A) was based on bending calculations. The rocket manufacturer recommends that attachment loads be concentrated at the nose of the rocket and at the nozzle attachment location. However, it is undesirable to attach to the nose and the nozzle of the rocket because of the bending it could experience during flight. This is illustrated in figure 21. With a rocket motor case thickness of 0.071 in. the rocket is predicted to have a maximum deflection of 0.263 in. and a maximum bending stress at ultimate load of 18,500 psi. This calculation was performed assuming that the length of the rocket was the length of the fuel only (L = 185 in.). A vertical acceleration of 2.2 *g* with a factor of safety of 2.25 was used based on a B-52 airplane captive-carry flight condition. The illustration in figure 21 demonstrates the simple loading case that was modeled in the calculations. With the above bending stress in mind, the forward attachment structure on the rocket was shifted back toward the FS193 bulkhead of the vehicle to alleviate bending. This forward attachment (A) on the rocket at FS193 of the vehicle has a reduced distance between the X-38 vehicle and the rocket casing, resulting in a stiffer support mount and a shorter load path to a large structural member inside the X-38 vehicle.

Shifting the forward attachment structure on the rocket back to vehicle bulkhead station FS193 meant that attaching the rocket would require clamping around the body of the rocket. Because the rocket bulges about 0.1 in. under thrust, the rocket manufacturer advised against attachment anywhere other than the above-mentioned forward (A) and aft (B) attachment points on the rocket. With the bending stress and bulging in mind, it was proposed to clamp around the rocket with a soft mount attachment. As shown in sections A-A and B-B of figure 22, a 0.375-in. bonded rubber pad interface is situated between the rocket and the aluminum mount. The rubber pad could be used to accommodate the bulging of the rocket. This concept was presented to the rocket manufacturer and it was determined to be a reasonable approach. Details of the proposed forward and aft mounting are further discussed in the next two subsections.

Forward External Attachment Structure

Figure 23 shows a conceptual design of the forward booster attachment structure (A) on the rocket for the forward attachment location, FS193. A soft-mounting clamp bolts around the rocket in two locations; at the top, denoted as A1 in the figure; and bottom, denoted as A2 in the figure. The clamp itself is made of 0.25-in. aluminum and is 12 in. long. This is a soft mount attachment, which implies that the structure will only take large loading in the y and z axes of the rocket. In order to react out the thrust of the rocket in the x-axis, two 0.25- by 1.5-in. steel straps were used. These straps attached to the loading point at the nose of the rocket and fixed to the forward attachment structure. The straps provide a load path directing the thrust at the nose of the rocket to the forward attachment structure (A). Drag loads on the rocket also need to be reacted

at the forward attachment structure (A). These loads are an order-of-magnitude less than the thrust and may be reacted by the rubber bond.

A detailed drawing of the forward attachment structure (A) is found in figure 22. The rocket attachment structure is connected to the vehicle at three points: two aft, denoted as A1 and A2 in the figure; and one forward, denoted as A3 in the figure. These attachment points consist of two explosive bolts in the aft position (A1 and A2) and one compression load pad in the forward position (A3). Jettison features are discussed below. Load bearing pads would need to be installed on the vehicle at the two aft attachment points (A1 and A2). These pads serve as a load path for the aft moment that the forward attachment structure of the rocket encounters in flight. A compression loading pad needs to be installed at the forward point (A3) to react out the thrust moment produced by the rocket. The aft attachment points (A1 and A2) serve as hard attachment points taking loading in the y and z axes.

Aft External Attachment Structure

The aft external attachment structure, denoted as B in figure 20, takes loading in the y and z directions but no thrust loads. This attachment was used as a pitch and yaw stabilizer fitting. Figure 24 shows a conceptual design for this aft attachment structure. The structure consists of a saddle fitting, the material of which is to be determined, with a Kevlar® (E.I. du Pont de Nemours and Company, Wilmington, Delaware) wrap to hold the saddle in place. The saddle structure connecting to the X-38 vehicle includes a frangible section that can be easily broken away. At jettison the rockets rotate about this frangible section until the fitting fractures, allowing the rockets to fall away from the vehicle without the vehicle incurring any damage.

Rocket Jettison Configuration

Normal jettison will be accomplished with the motor thrust near zero and with the motor weight near 450 lb. Two explosive bolts (A1 and A2), shown in figures 23 and 25, will be blown followed by the firing of an ejector piston to start the rocket cases rotating outward into the air stream. The aft external rocket case attachment structure (B) will be designed to remain attached until it rotates through an angle on the order of 30 deg to 45 deg, at which time the connection will fracture because of bending and tension at the machined frangible section. The aft external attachment structure will guide the rocket case to avoid recontact with the flight vehicle during initial stages of separation. With the proper ejector piston the forward attachment structure (A) can be designed to separate even if only a single explosive bolt fires. The frangible aft attachment will separate properly even if the rocket case were to pitch up or down.

Preliminary Loads

With the above conceptual design in mind, a set of design loads was developed. Several different flight configurations have been considered including captive-carry, zero thrust with the pre-fire weight of the rocket, full thrust, and zero thrust with the post-fire weight of the rocket. For each flight configuration several flight conditions were considered. Of the considered flight conditions one or two cases were singled out as providing worst-case loading. The loads were derived using

the dimensions shown in figure 26. The loads assessment was performed before the final toe-out and pitch angles were determined. It was assumed that toe-in angle on the rocket is zero and the rocket pitch angle is 11 deg nose-up. All aerodynamic data used in the calculations was taken directly from the nonlinear simulation. Structural dynamics of the XTRA configuration have not been completed.

Design Loads

Design loads were derived by taking the maximum magnitude loading at each attachment point and in each direction. As shown in figures 24 and 25 of the forward (A) and aft (B) attachment structures, the X-38 vehicle internal structure will need to be strengthened. This internal strengthening will be designed and completed by the outside contractor. A factor of safety of 2.25 (standard for metallic structures) was then applied. The design loads are listed in table 7. Rocket buckling calculations were not performed for this study.

Table 7. Design loads including factor of safety.

Final design loads
(Factor of safety = 2.25)
Ax = 763.5
Ay = 1923.4
Az = 3930.1
Fx = 53362.0
Fy = 5529.9
Fz = 20925.2

Vehicle Clearances

The addition of rockets to the X-38 vehicle had the potential to create clearance problems. Two primary vehicle clearance issues were identified and are examined below.

Ground Clearance

Installing the rockets at a moderate incidence angle (up to 11 deg) gives rise to a possible overhang of the rocket below the belly of the X-38 vehicle. This prompted an examination into the amount of clearance that will be available between the belly of the X-38 vehicle and the ground at takeoff. This study was performed assuming worst-case takeoff and landing conditions for the B-52 airplane: tires and oleo struts flat on the right side, right tip protection gear in contact with the ground, and the airplane rolls during landing. It was determined that there will be 12 in. of clearance between the belly of the X-38 vehicle and the ground.

Access Panels

A mock-up of the rockets on the X-38 vehicle was constructed to address any issue including clearance with the proposed rocket attachment configuration. As can be seen in figure 27 the access door was slightly obstructed. Technicians were consulted and it was determined that there was an ample amount of room for a person to climb in and out of the X-38 vehicle and allow for quick crew exit during a ground emergency. Because the access doors will need to be accessible up to the time of flight, the rockets will already be attached to the vehicle when final preflight procedures are conducted. A set of operating procedures will need to be developed and training provided in order to work around the rockets. Clearance for access to the side panels was increased with rocket toe-out.

Structural Conclusions

A conceptual design of the XTRA structural modifications has been completed. To avoid excessive bending, the motors are attached at FS193 and the aft bulkhead of the X-38 vehicle. Attachment hardware loads are carried into major structural members. The forward attachment structure (A) on the rocket has a soft clamp with a rubber interface to allow rocket bulging during the burn. Rigid straps carry thrust loads from the nose of the motor to the forward attachment structure (A). Two explosive bolts (A1 and A2) and an ejector piston are used to jettison the motor from the X-38 vehicle. The aft attachment structure (B) on the rocket carries no thrust loads, but y- and z-axis movements are constrained. A frangible section is designed to break as the motor rotates away from the X-38 vehicle during the jettison sequence. A mock-up of the motor was used to verify the installation design and ensure crew access during preflight operations.

THERMAL CONSIDERATIONS

Two primary thermal considerations exist for the X-38 transonic boost configuration: cold soak of the solid rockets beyond their operating specifications, and plume-induced heating of the base and aft control surfaces of the X-38 vehicle. These are discussed in the three subsections below.

Cold Soak of the Rocket Motors

The manufacturer's specified operating temperature limits for the rocket motor range from –10 °F to +125 °F. One concern for the operation of these rockets is that the long duration climb of the B-52 airplane to launch altitude may cause the rockets to cold soak to an extent that the operating limits are exceeded. This subsection describes the analysis methods used to perform the cold-soak analysis, and the resulting rocket temperature predictions.

Cold-Soak Analysis

Thermal analyses use the actual trajectory flown by the B-52 airplane during V132 captive-carry flight 002 to predict the vehicle climb rate and variations in atmospheric properties during the climb to altitude. The Mach number and altitude profiles for this flight are shown in figure 28. During the flight, the B-52 airplane climbed to an altitude of approximately 30,000 ft and lingered

there for approximately 30 min while trying to debug an actuator problem on the X-38 vehicle. After this period, the vehicle climbed to the simulated launch altitude of 46,000 ft.

Because the vehicle lingered at an altitude of 30,000 feet instead of climbing directly to the launch altitude, it is believed that the results of the cold-soak analysis using this trajectory are conservative.

The cold-soak analysis was first performed as a transient lump-sum (ref. 4) analysis in which the heat flux into the rocket mass was assumed to occur uniformly along the rocket surface and the mean-mass rocket temperature was predicted. Cooling of the rocket's outer shell was analyzed using a monolithic slab method (ref. 5) with a lump-sum estimate for the mean heat flux multiplied by a safety factor of 1.5. These two temperature prediction methods were used together to assess the thermal operating margins for the rocket.

Figure 29 shows the results of the cold-soak analysis performed using the trajectory of the second captive-carry flight. The upper plot shows time histories of the ambient temperature, T_∞; stagnation temperature, TT2; adiabatic wall temperature, TA_WALL; the predicted bulk mass temperature, TBULK; and the predicted external wall temperature, TWALL; starting from an initial temperature of 80 º F (572 ºR). The lower operational temperature limit (–10 º F) (482 ºR) for the rocket is also shown. In the lower plot of figure 29, the heat transfer rates are plotted. The convective, radiative, and total heat loss rate from the outer casing is plotted and compared with the total heat transfer rate from the inner mass of the rocket to the outer casing. Notice that the heat lost from the outer wall is greater than the heat being transferred from the internal mass to the rocket skin. The result is that the outer wall cools slightly faster than the internal mass of the rocket. In both cases, however, there is still a comfortable margin between the rocket temperatures and the operational limit of the motor.

Figure 30 compares the bulk wall temperature of the rocket and the total heat loss rate at the surface for several different starting temperatures. Notice that the rockets cool at a slower rate for the lower initial temperatures (Tinits); however, the higher starting temperatures still result in a greater temperature margin (above the operational limit). Any starting temperature above 60 ºF (552 ºR) provides a reasonable temperature margin. By eliminating the data from the long altitude hold of the B-52 airplane on flight 002, starting temperatures below 20 ºF (512 ºR) remain within the operational limits for ignition.

Rocket Plume Heating

A lumped-mass analysis was used to compute the rocket plume heating effects on the base region of the X-38 vehicle. The rocket plumes were modeled by unit-radius incandescent spheres radiating at the rocket plume temperature. An "inverse-square law" diminishment of the radiant energy from the unit was modeled. The total energy flux impinging on the base was evaluated by integrating the inverse square law along the width and breadth of the base (ref. 6). Back radiation to ambient and convective heat loss at the base were modeled. The base material is assumed to be a type "S" fiberglass (ref. 7). Two predicted curves for the base temperature with and without a reflective heat shield were evaluated. Time histories of the base temperatures are shown in

figure 31. The unshielded base wall temperature becomes dangerously high during the rocket burn. On the other hand, the shielded base area remained moderately cool.

Because the rocket plumes are assumed to radiate directly onto the base area with no shielding by the rocket nozzles, it is believed that the radiation analysis presented in this section is conservative. However, it must also be acknowledged that the monolithic analysis does not allow for the effects of localized heating and it may also be possible for some of the hot rocket exhaust gas to be recirculated into the base region. This would have the effect of reducing the amount of convective cooling that occurs along the base. Considering the high predicted peak temperature for the unshielded base, and recognizing that the lumped-mass analysis performed in this section has limitations, it was recommended that the base area of the X-38 vehicle be fitted with a reflective heat shield.

GROUND TESTS

To minimize risk, numerous ground tests were considered for the XTRA effort. The following tests were considered:

1. A wind tunnel test (recommended)
2. A rocket pressure–bending test (recommended)
3. A captive-carry flight (recommended)
4. An ignition and flight termination system tests (recommended)
5. A ballast dump–jettison test (recommended)
6. A hook loads test (recommended)
7. A rocket jettison test
8. A ground vibration test
9. A static loads test of attachment hardware.

Primary Ground Tests

The six primary ground tests discussed below were considered important for the success of the XTRA flight-test program.

Wind Tunnel Test

A wind tunnel test would be required to document the aerodynamics, control effectiveness, and rocket attachment loads. Preflight analysis tools are not sufficient for estimating the drag, lift, pitching moment, lateral–directional, or control effectiveness changes caused by the addition of the external rocket payload. The wind tunnel test would also provide an opportunity to design an aerodynamic fairing between the rocket and the X-38 vehicle for increased performance. The updated aerodynamic model would be used to verify the performance and stability of the XTRA configuration with the V201 control laws.

Rocket Pressure–Bending Test

Because the rocket is attached at forward and aft locations, bending loads while the rocket is burning are a concern. Excessive bending could lead to cracking or separation of the solid rocket core. These risks could be mitigated by testing, possibly by having the manufacturer introduce bending loads during the normal empty core pressure test that is done on every rocket shell.

Captive-Carry Test

The XTRA configuration would require a captive-carry flight on the B-52 airplane, primarily to investigate loads and vibration. Cold-soak data on the motors could also be recorded.

Ignition and Flight Termination System Tests

All new electronic and fiberoptic systems would be fully tested. Tests to verify proper ignition and flight termination system (FTS) commands would be performed. These tests do not require the actual pyrotechnics to be initiated.

Ballast Dump–Jettison Test

The water ballast dump system or the alternate ballast jettison system, required to maintain proper CG control, would be thoroughly tested prior to flight. If a water system is selected, it can also be exercised on the captive-carry flight.

Hook Loads Test

The X-38 hook loads with the required margins are expected to be higher than has been previously proof tested. For this reason a hook loads test is recommended.

Secondary Ground Tests

The three secondary ground tests discussed below are not considered a requirement for preparation of the XTRA configuration for flight.

Rocket Jettison Test

The rocket jettison test would be used to test the explosive bolts, ejector cartridge, and jettison hardware. The rocket mock-up tubes described above could be weighted to simulate the empty rocket weight. However, without the aerodynamic loads from flight, the jettison may not provide any significant information on the acceptability of the design.

Ground Vibration Test

Preliminary analysis of the structural modes of the XTRA configuration suggests that sufficient flutter margins exist to safely forego a ground vibration test (GVT).

Attachment Hardware Static Loads Test

The rocket motor attachment hardware design has large margins of safety. As a result, static loads testing would probably not be required.

LAUNCH–RANGE OPERATIONS

The X-38 transonic boost configuration would use the same launch procedures and resources as the standard X-38 vehicle. The expected launch altitude is 46,000 ft. Extended delays after the B-52 airplane begins to climb would not be tolerated because of the thermal cold-soak concerns described above. It is recommended that thermocouples be used on or in the rockets to ensure the rocket temperatures are within specifications before launch. Release from the B-52 airplane would follow standard procedures. The additional weight of the rockets would result in a quicker separation between the B-52 airplane and the X-38 vehicle after release. There are no known additional risks that would allow a collision of the X-38 vehicle with the B-52 airplane.

An extended range would be required to support the rocket-assisted operation. Discussions with NASA DFRC and Air Force Flight Test Center (AFFTC) range safety teams resulted in the preliminary identification of an acceptable range within the Edwards Air Force Base complex. Although the nominal trajectory would easily stay within the range, possible failure cases could result in an impact outside the range. Possible range violation scenarios include premature jettison or structural failure leading to free flight of a solid rocket booster or asymmetrical ignition of a single solid rocket on the X-38 vehicle. To mitigate these risks an FTS would be required for the boosters. The TTS blows two holes near the front of the rocket that terminate thrust generation by eliminating the chamber pressure. The rocket-based TTS should have two actuation modes. First, while attached to the X-38 vehicle, the rocket TTS should be controlled by the range safety officer on the ground. Second, to prevent unexpected flyaway of the rocket, a lanyard should be used to trigger the TTS shortly after or during rocket separation—for any reason—from the X-38 vehicle. The rocket TTS should not be enabled until the rockets have been ignited to avoid accidental TTS firing while attached to the B-52 airplane.

Many new operational and emergency procedures will be written to mitigate hazards unique to the XTRA configuration. These procedures will include both ground and flight concerns.

CONCLUSION

The current X-38 transonic boost design is capable of obtaining aerodynamic data at Mach numbers up to 1.5. The best configuration for the task combines Vehicle 131R with two side-mounted Black Brant Mk1 solid rocket motors. The nozzle exit plane extends about 35 in. aft of the X-38 vehicle base to avoid plume impingement. The rockets are in a nose-up attitude with respect to the X-38 vehicle reference axis so that the thrust line is close to the center of gravity and a portion of the rocket thrust is used to augment the vehicle lift for the pull-up maneuver. The rockets are attached at two points with rigid straps carrying the thrust loads from the rocket nose to the central mount. An off-the-shelf thrust termination capability can be included on the rockets to terminate the thrust for range safety. This feature blows holes near the nose of the rocket. Explosive bolts and

an ejector are used at the forward mount to jettison the rockets after burnout. The aft attachment has a frangible section that severs as the forward mount is ejected and the rocket rotates away from the aircraft. Very little external hardware will remain after jettison so that clean aerodynamic data can be obtained, using the existing PTI system to perform maneuvers.

Approximately 780 lb of ballast is required to be relocated to the forward bay and an additional 725 lb must be added at the same location to balance the center of gravity to an acceptable position. After rocket jettison and before parafoil deployment, 800 lb of the ballast must be deployed, either by the jettison of a metallic plate or by the dumping of water.

The flight control system would require modification to enable control of the rocket ignition and of the rocket–ballast jettison. Loss-of-control logic may need to be modified. Because of rocket fuel burn and jettison, vehicle mass properties and aerodynamics change over the course of the flight. Additional modifications to the control system will likely be required to account for these effects.

The solid rocket is limited to a lower temperature of –10 °F. Analysis has shown that the thermal mass of the rocket is sufficiently high that these lower temperatures are not reached for a nominal or extended B-52 airplane climb profile for ground temperatures of 20 °F or above. Base heating (caused mostly by radiation) could pose a problem and a more detailed analysis may confirm that some shielding on the base and control surfaces will be necessary.

The modified V131R configuration would weigh close to 24,000 lb, which is over the current pylon limit. The pylon, however, must be modified regardless of the XTRA program, in order to support the 25,000-lb V133 flight-test vehicle. All jettisoned items would fall in government-owned, controlled areas and the X-38 vehicle would land on a dry lakebed.

As expected, the configuration has additional risks over the baseline X-38 vehicle. Failure of either of the rockets to ignite would result in an immediate departure. It is not clear whether thrust termination, jettison of the rocket, and emergency deployment of the parafoil or backup chute would save the airframe. Other anomalies such as failure of a ballast jettison system or failure of the post-burn rocket jettison are probably not catastrophic. The XTRA configuration is resistant to three-sigma start-time and thrust dispersions. As currently defined, large burn-time dispersions produce unacceptably large roll disturbances. The rocket manufacturer was consulted to potentially reduce the burn-time dispersion based on special XTRA characteristics.

Programmed test inputs are capable of producing about three parameter identification maneuvers at Mach numbers above sonic and about five maneuvers between Mach 0.8 and Mach1.0 on each flight. The maneuvers are of acceptable quality for parameter identification, although the Mach number is bleeding off because of the climbing trajectory required by the dynamic pressure limit. Lift, drag, and control surface trim position data can also be extracted throughout the trajectory. A relaxed dynamic pressure limit could allow a trajectory with additional data collection time.

Dryden Flight Research Center
National Aeronautics and Space Administration
Edwards, California, October 2, 2002

REFERENCES

1. Reed, R. Dale, *Wingless Flight: The Lifting Body Story*, NASA SP-4220, 1997.

2. Sutton, George P., *Rocket Propulsion Elements: An Introduction to the Engineering of Rockets*, Sixth Edition, John Wiley & Sons, Inc., New York, 1992.

3. Chemical Propulsion Information Agency, *Rocket Motor Manual, Volume I,* CPIA/M1, Johns Hopkins University, Columbia, Maryland, 1996. Requests for this document shall be referred to the Naval Air Warfare Center Weapons Division, Code477000D, China Lake, California, 93555-6100.

4. White, Frank M., *Heat and Mass Transfer*, Addison-Wesley Publishing Company, Inc., Reading, Massachusetts, 1991.

5. Carslaw, Horatio Scott, and J. C. Jaeger, *Conduction of Heat in Solids*, Second Edition, Oxford University Clarendon Press, London, 1959.

6. Rade, Lennart, and Bertil Westergren, *Beta Mathematics Handbook*, Second Edition, CRC Press, Boca Raton, Florida, 1990.

7. Watson, James C., and N. Raghupathi, "Glass Fibers," *Engineered Materials Handbook, Volume 1: Composites*, ASM International, Metals Park, Ohio, 1987.

FIGURES

EC99-45080-25

Figure 1. Flight test of X-38 Vehicle 132.

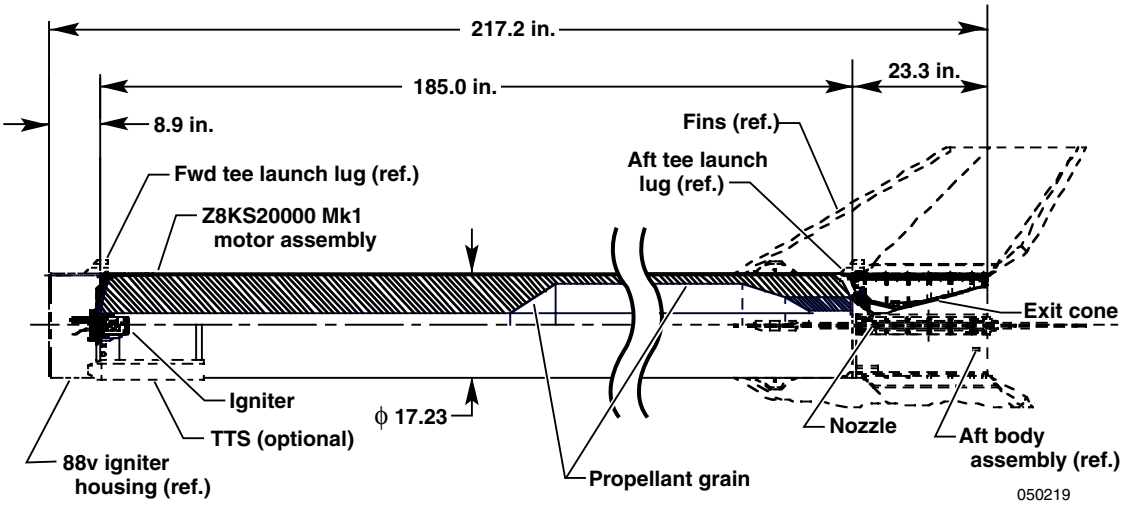

Figure 2. Black Brant Mk1 rocket motor, from Black Brant system data sheet, 26KS20000 Mk motor (Bristol Aerospace Ltd., Winnipeg, Manitoba, Canada).

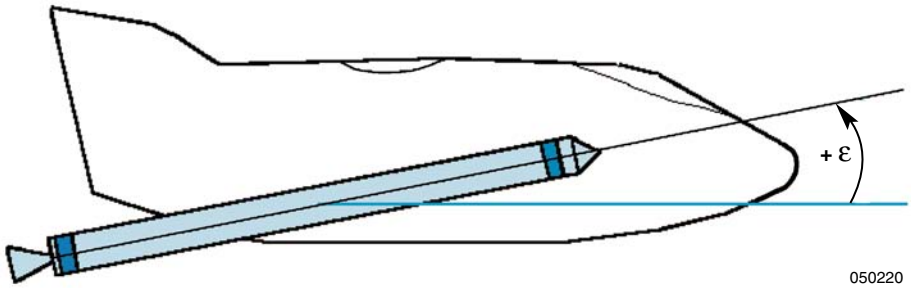

Figure 3. Vehicle 131 right side view showing the pitch installation angle, ε.

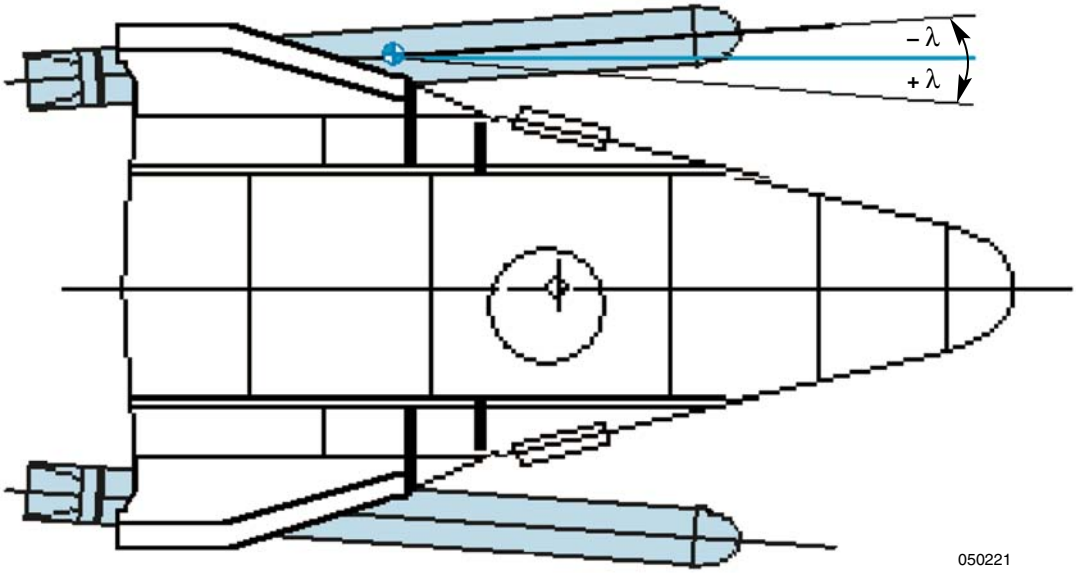

Figure 4. Vehicle 131R top view showing the yaw installation angle, λ.

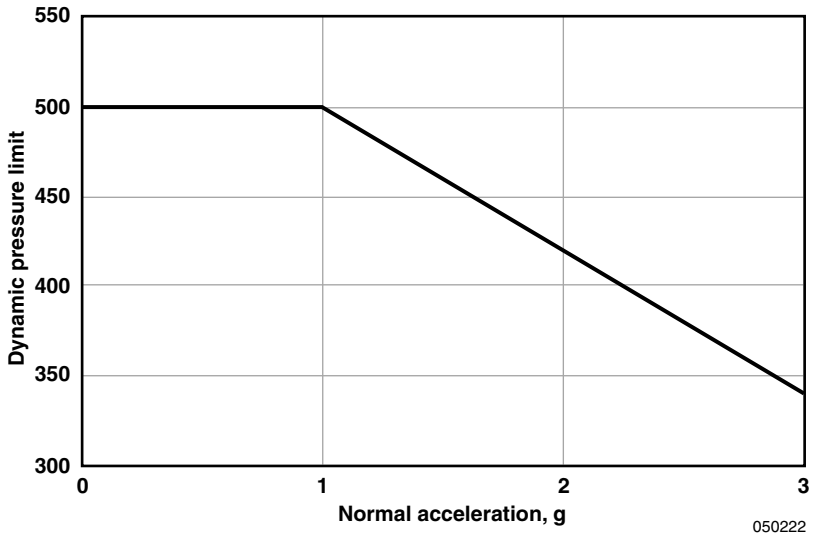

Figure 5. Dynamic pressure limit used for simulation studies.

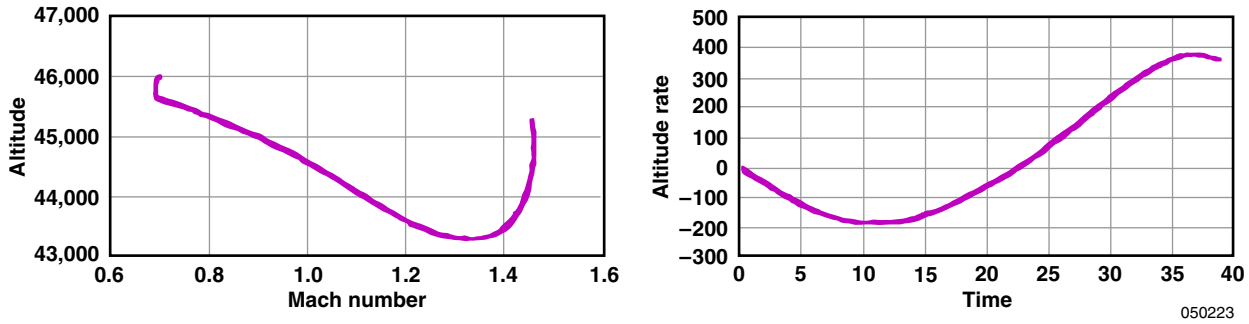

Figure 6. Altitude compared with Mach number, and altitude rate time history for rocket burn segment, $\varepsilon = 0$ degrees.

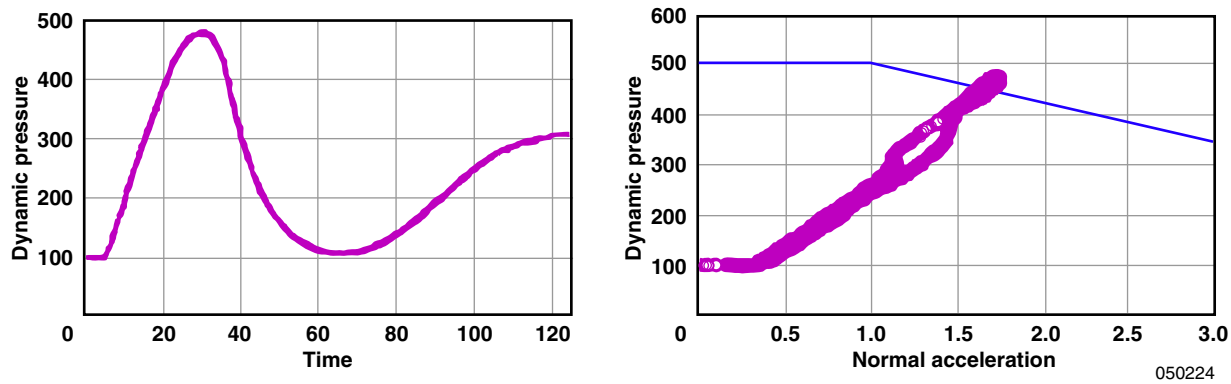

Figure 7. Dynamic pressure time history, and dynamic pressure compared with load factor, $\varepsilon = 0$ degrees.

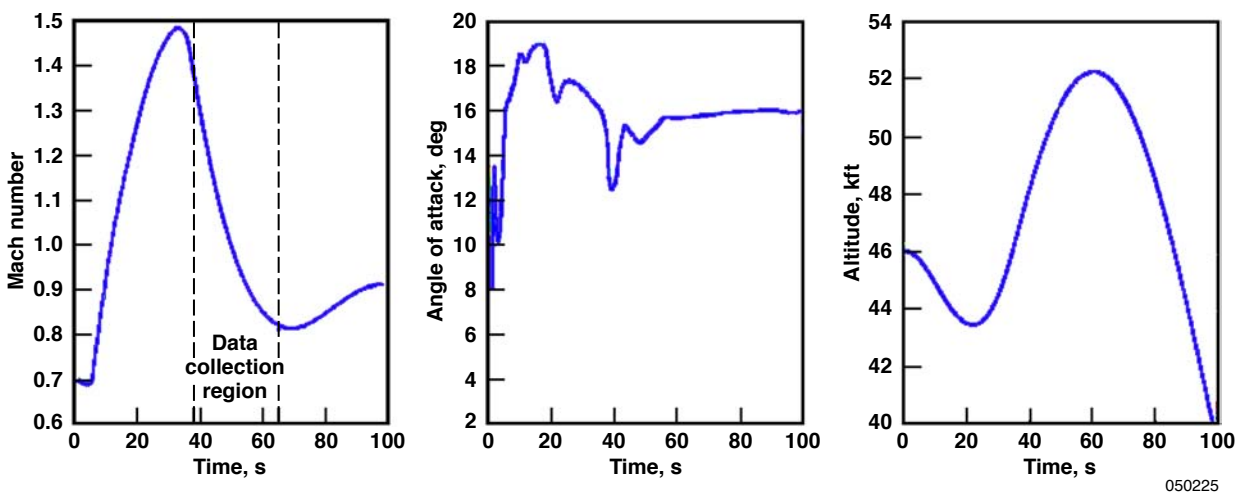

Figure 8. Mach number, angle of attack, and altitude time histories, $\varepsilon = 0$ degrees.

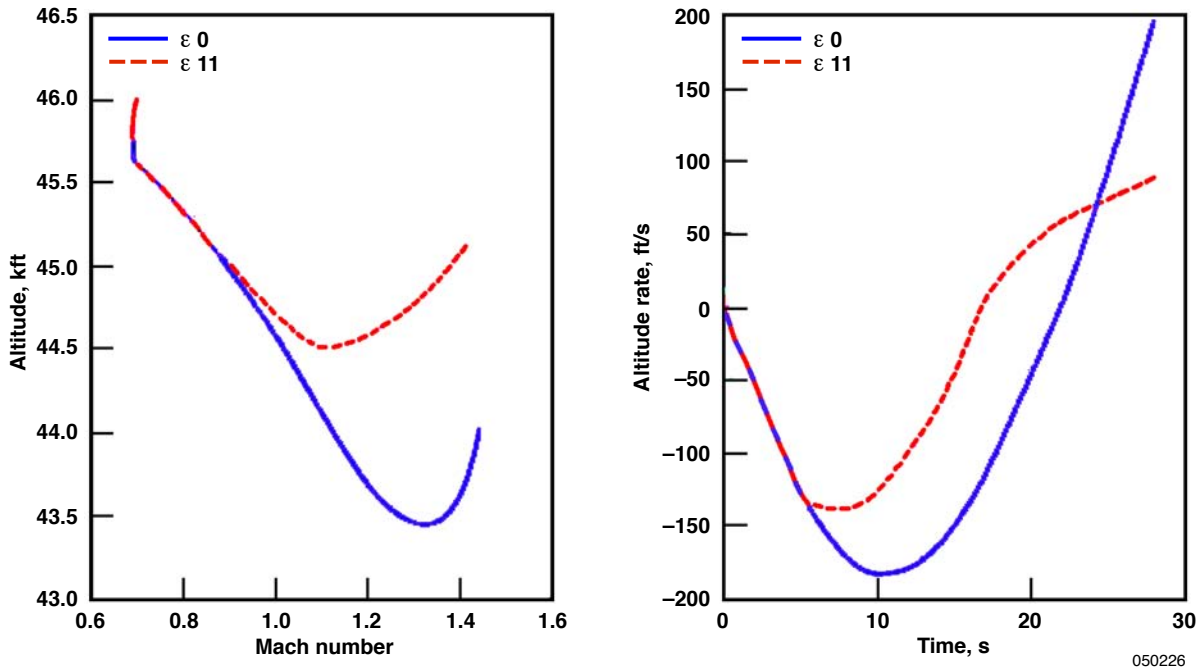

Figure 9. Altitude compared with Mach number, and altitude rate, showing the effect of increased pitch installation angle on climb initiation.

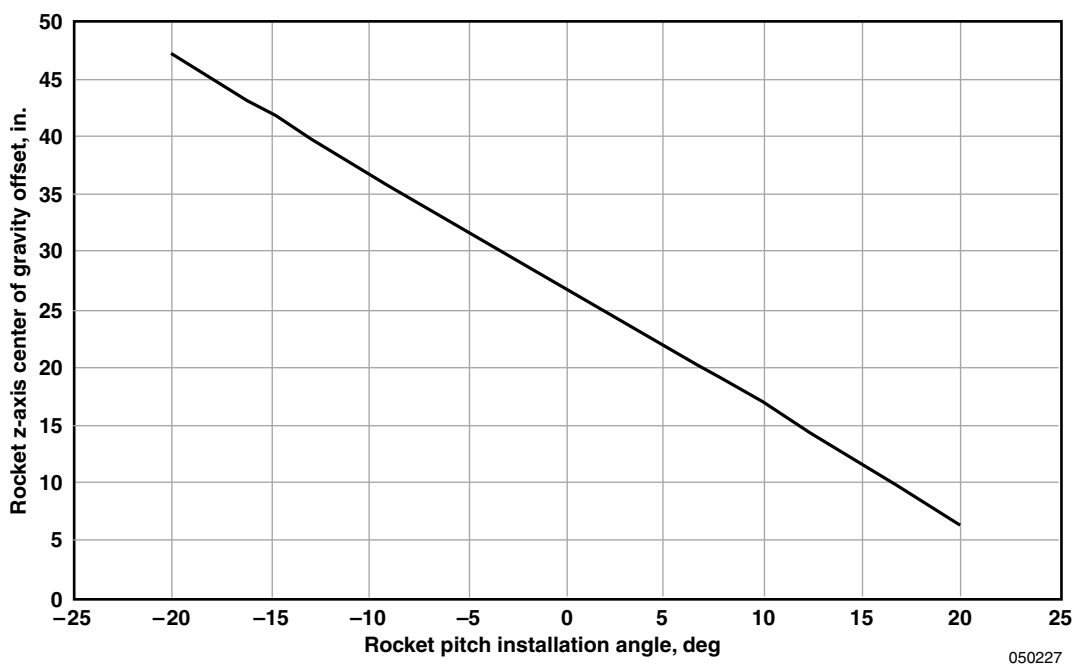

Figure 10. Approximate rocket Z-CG offset from vehicle CG for zero pitching moment.

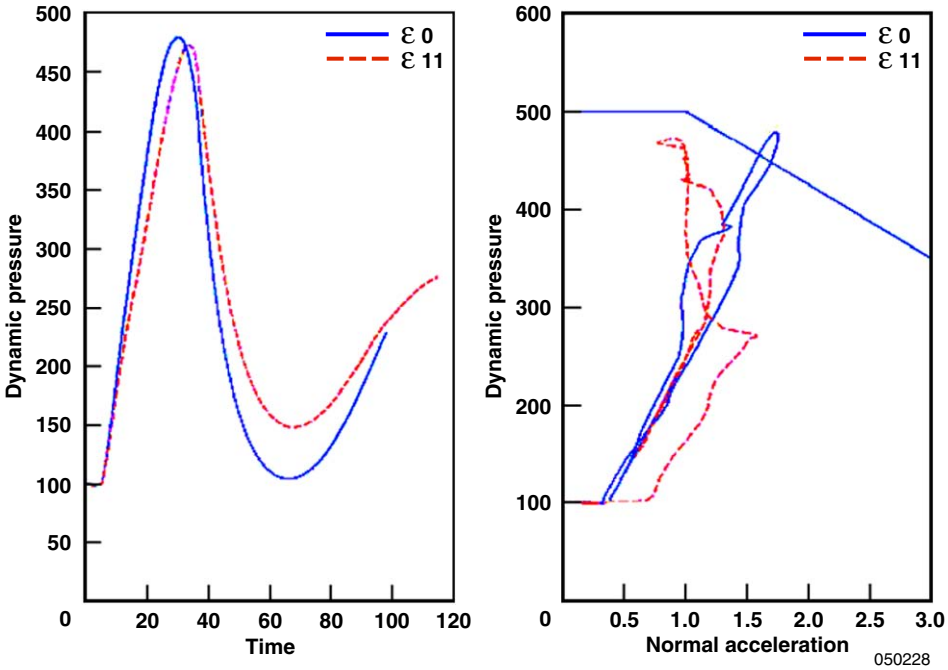

Figure 11. Dynamic pressure compared with time and load factor, showing the effect of pitch installation angle on lowering dynamic pressure.

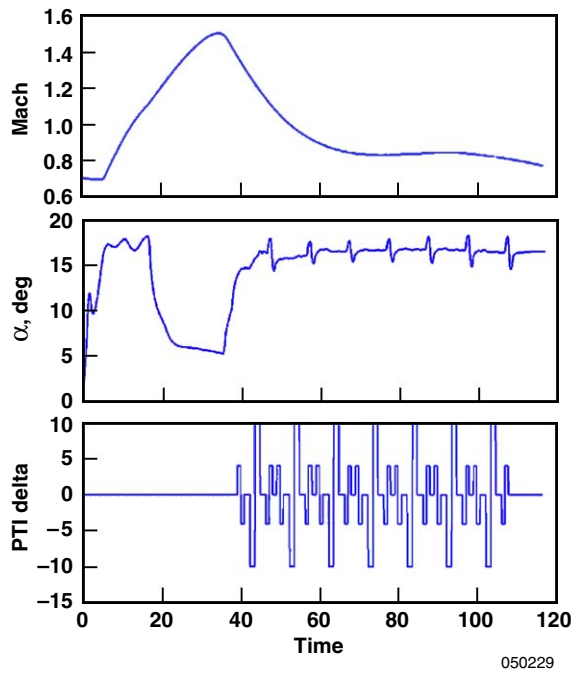

Figure 12. Sample trajectory illustrating the use of programmed test inputs.

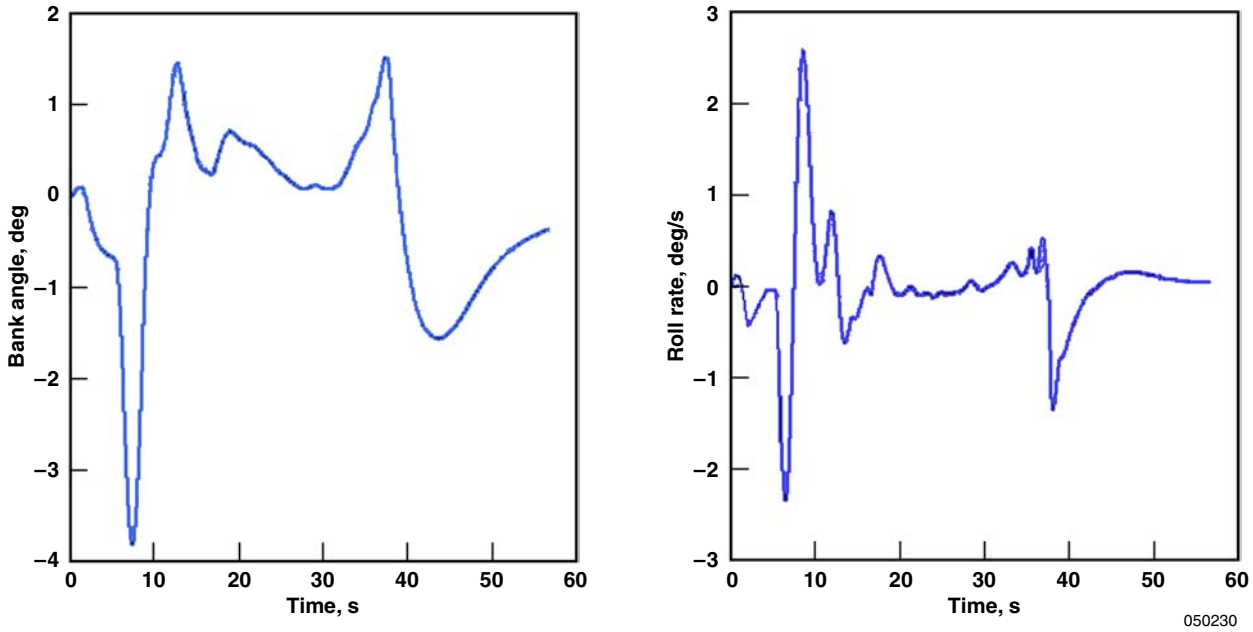

Figure 13. Simulation results showing the effect of a three-sigma thrust dispersion.

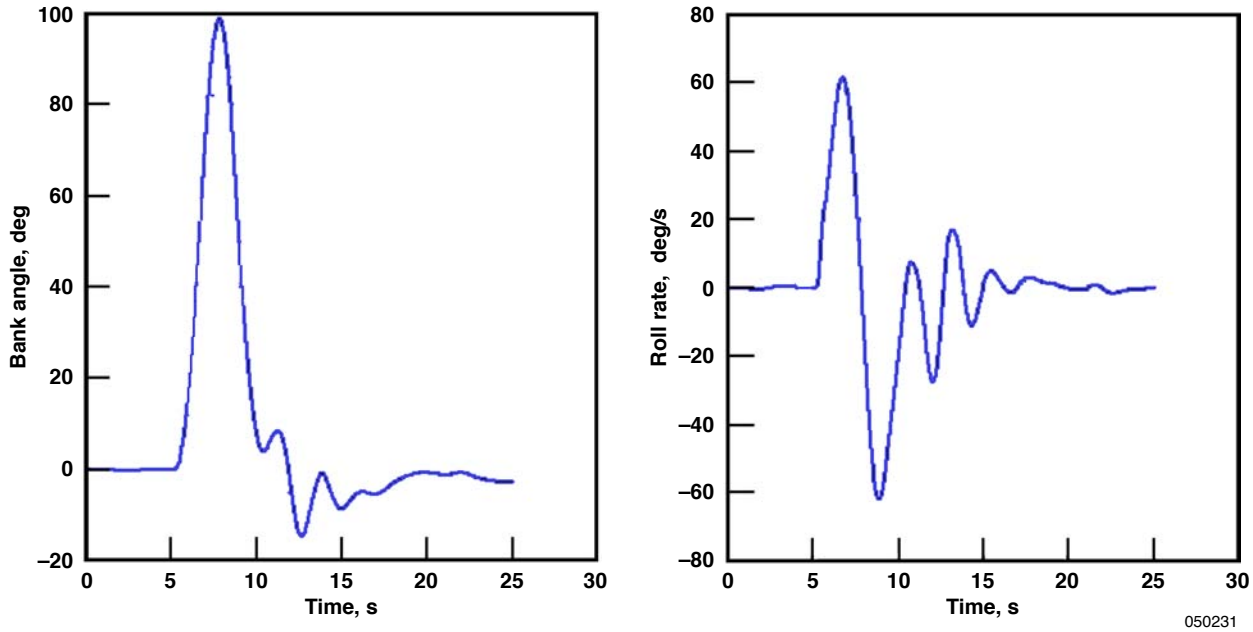

Figure 14. Effect of three-sigma rocket ignition time dispersion on bank angle and roll rate.

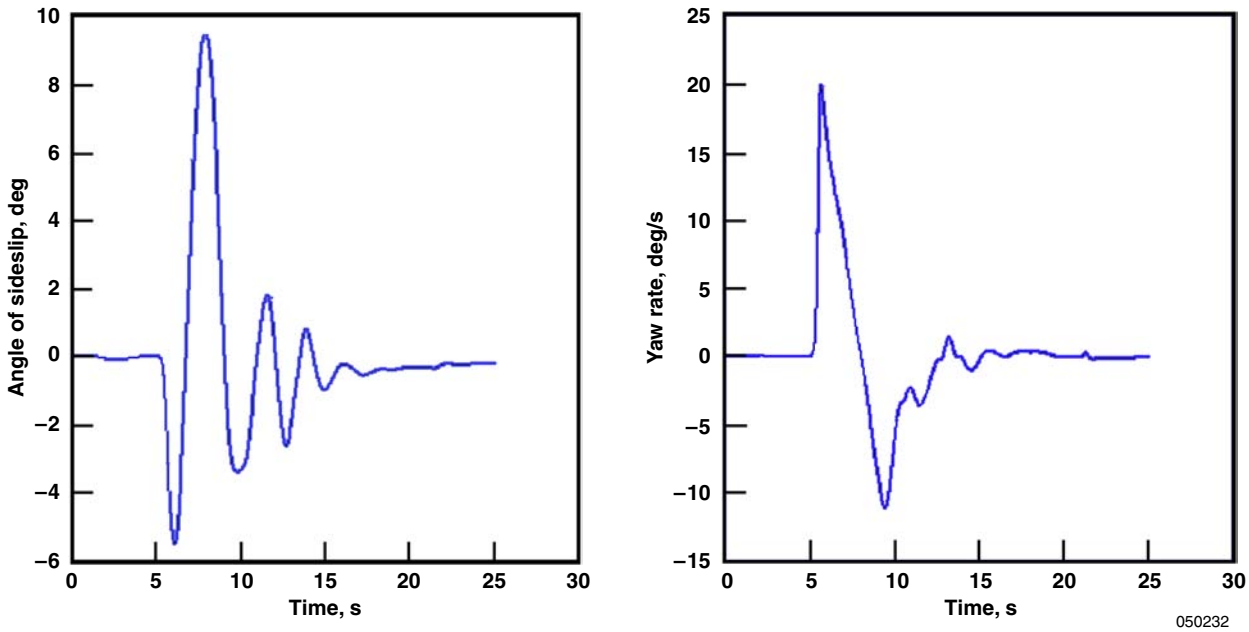

Figure 15. Effect of three-sigma rocket ignition time dispersion on sideslip and yaw rate.

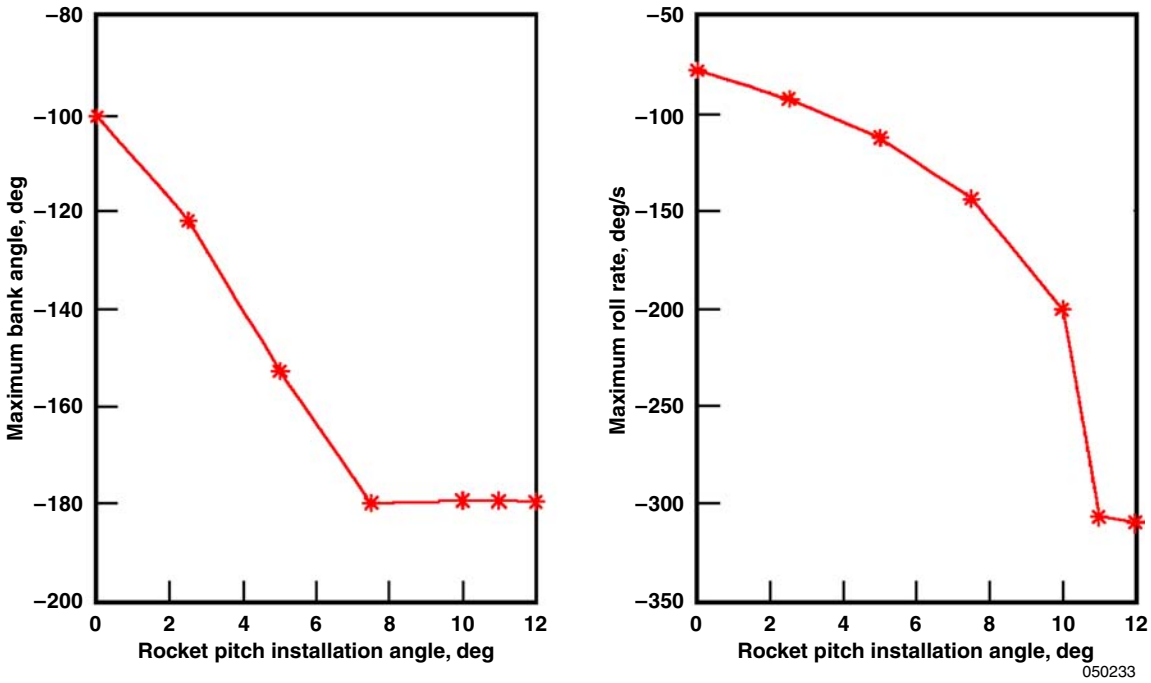

Figure 16. Roll rates and bank angles resulting from a three-sigma burn-time dispersion for various rocket pitch installation angles.

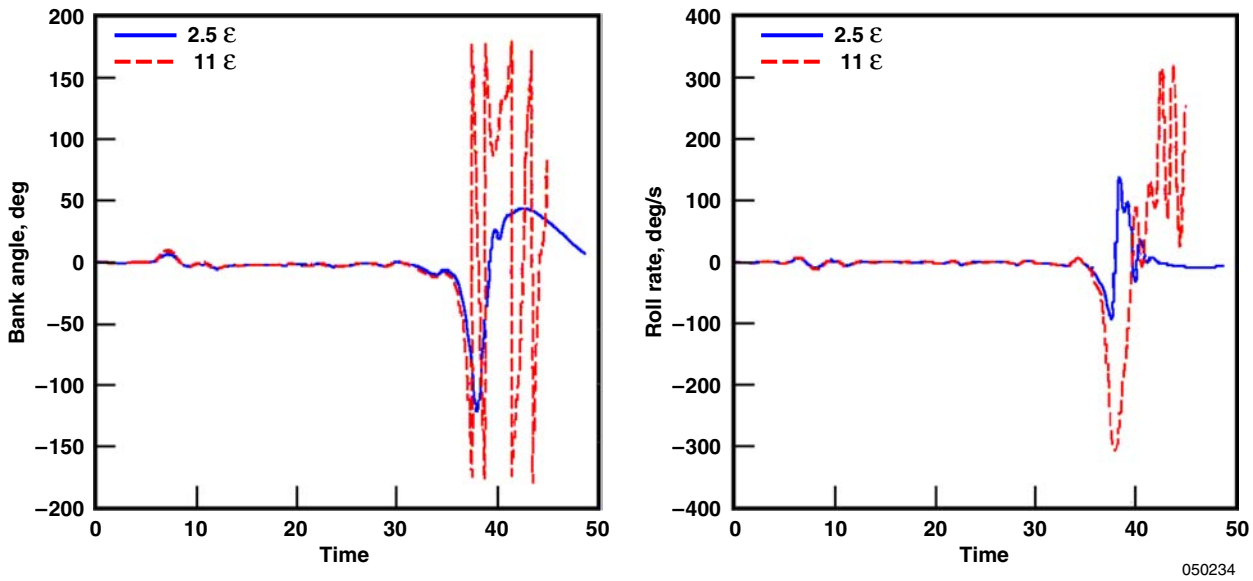

Figure 17. Effect of pitch installation angle on vehicle response to a three-sigma burn-time dispersion.

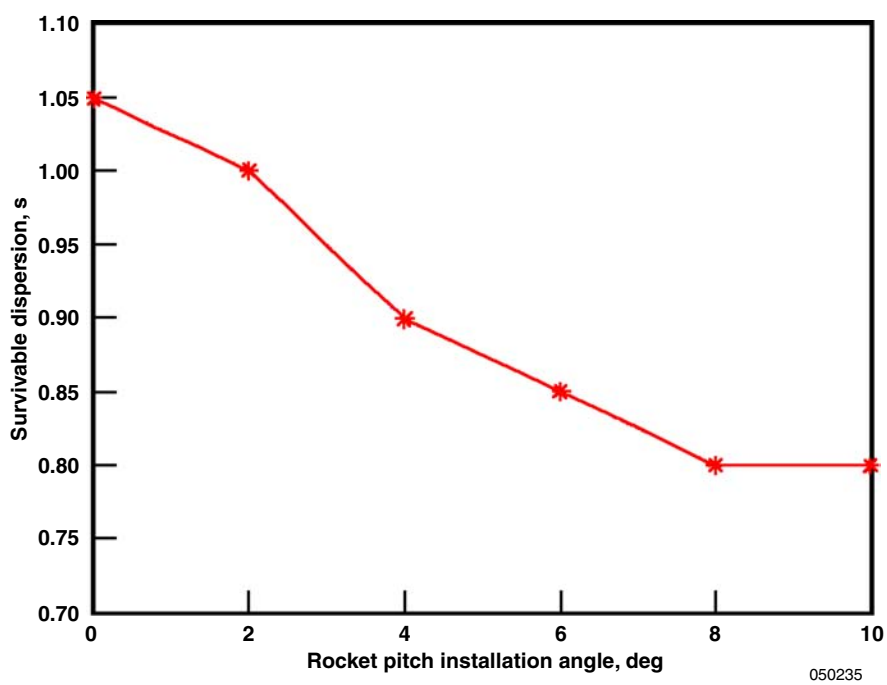

Figure 18. Effect of pitch installation angle on maximum survivable burn-time dispersion.

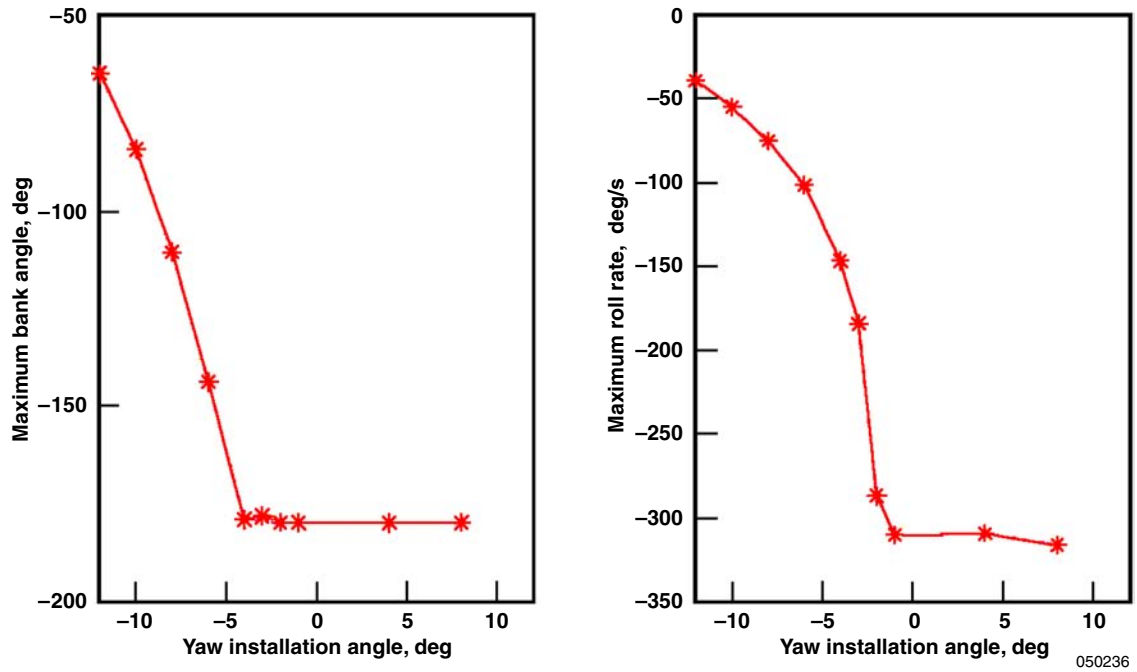

Figure 19. Effect of yaw installation angle on the vehicle response to a three-sigma burn-time dispersion $\varepsilon = 11$ degrees.

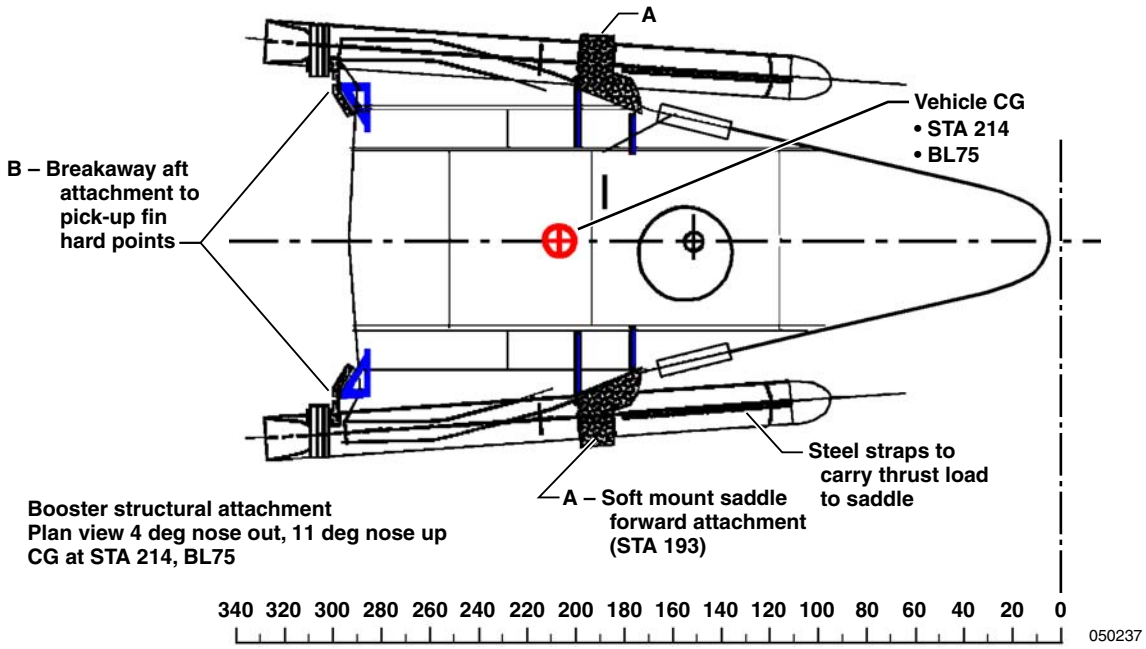

Figure 20. Rocket attachment structure conceptual design.

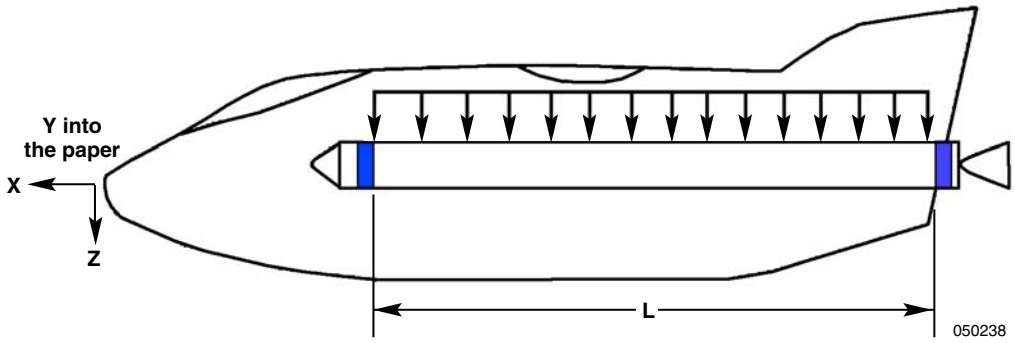

Figure 21. Loading case for a forward and aft mount attachment.

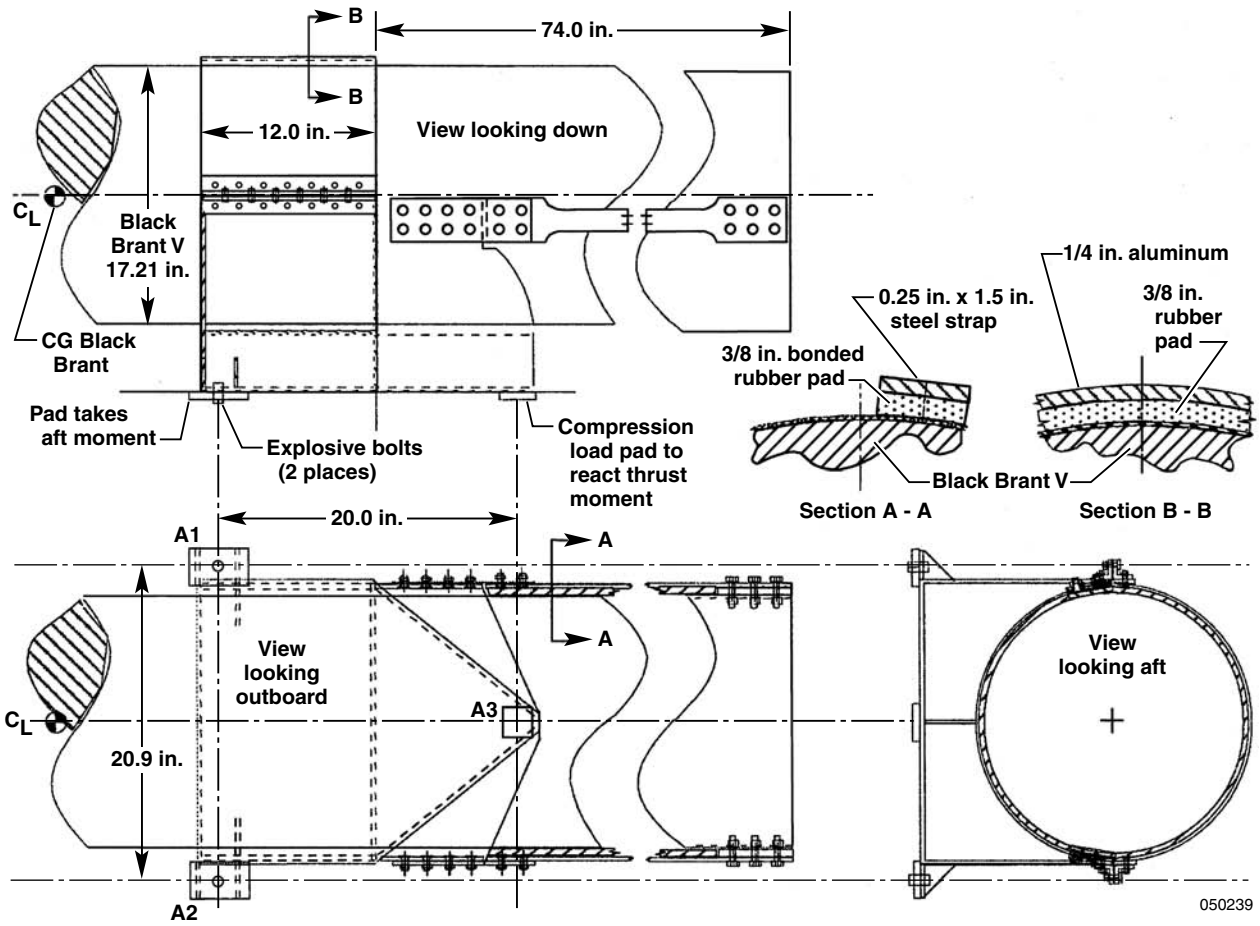

Figure 22. Forward attachment structure and thrust strap.

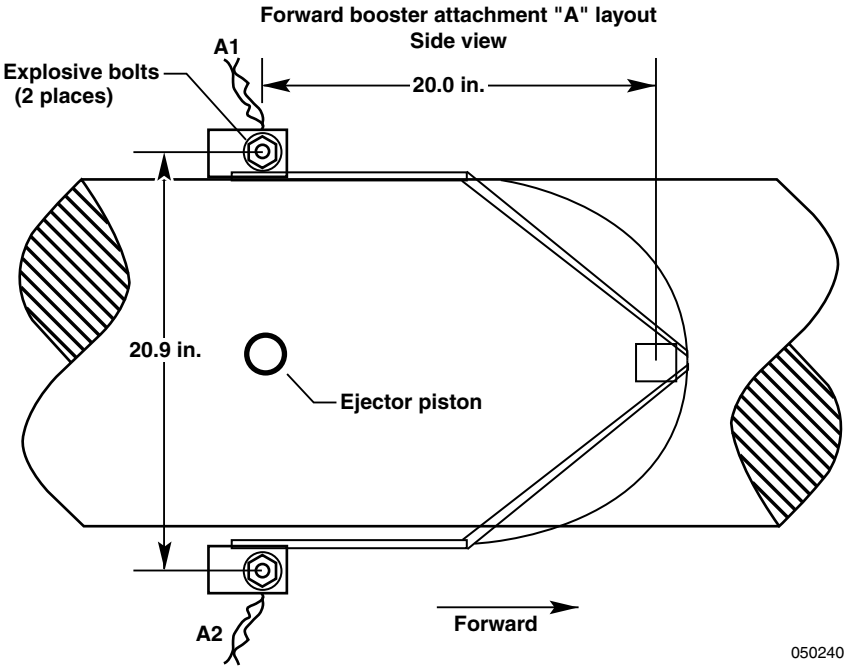

Figure 23. Forward attachment structure—vehicle interface conceptual design, side view.

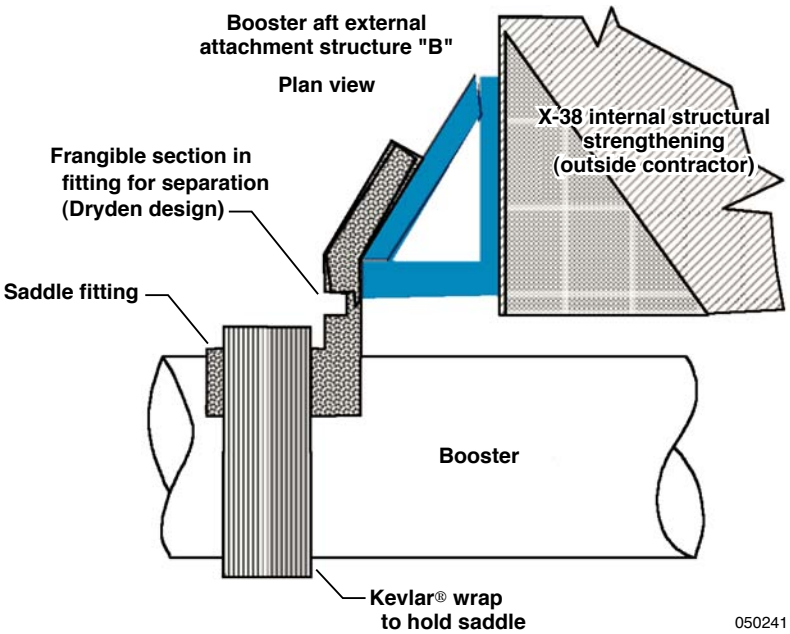

Figure 24. Aft attachment structure conceptual design.

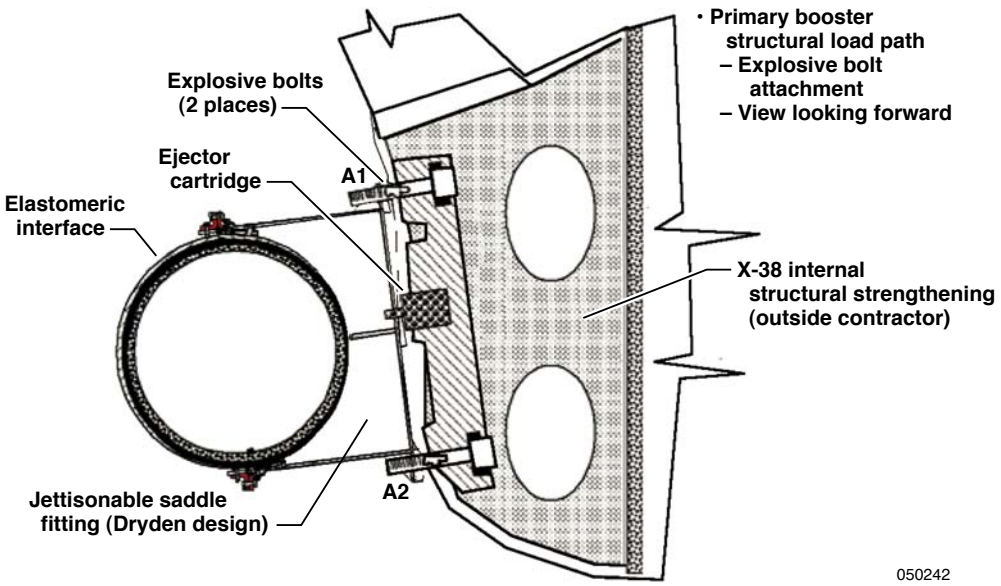

Figure 25. Forward attachment cross-section showing jettison systems.

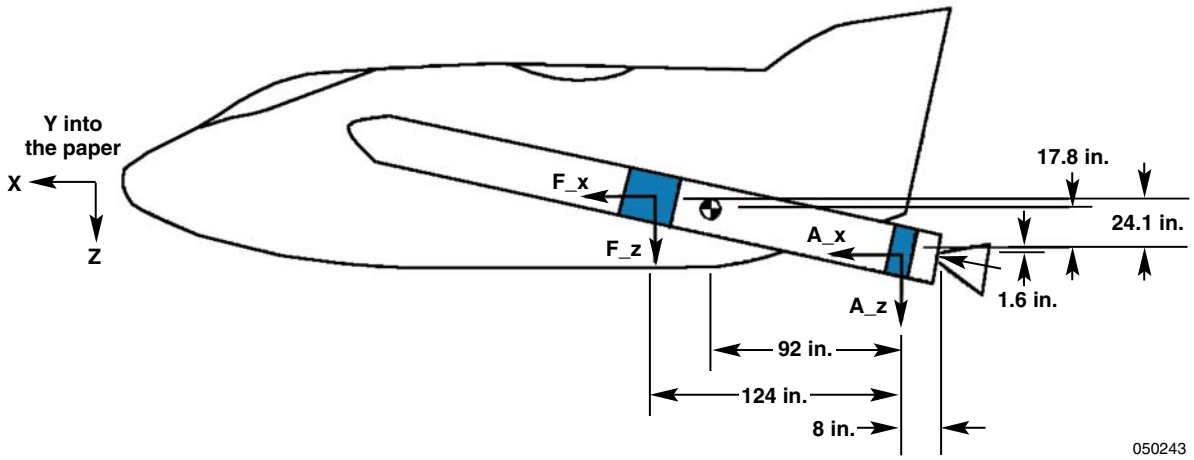

Figure 26. Dimensions used in loading calculations.

Figure 27. Mock-up rocket motor installation illustrating crew access, $\varepsilon = 11$ degrees.

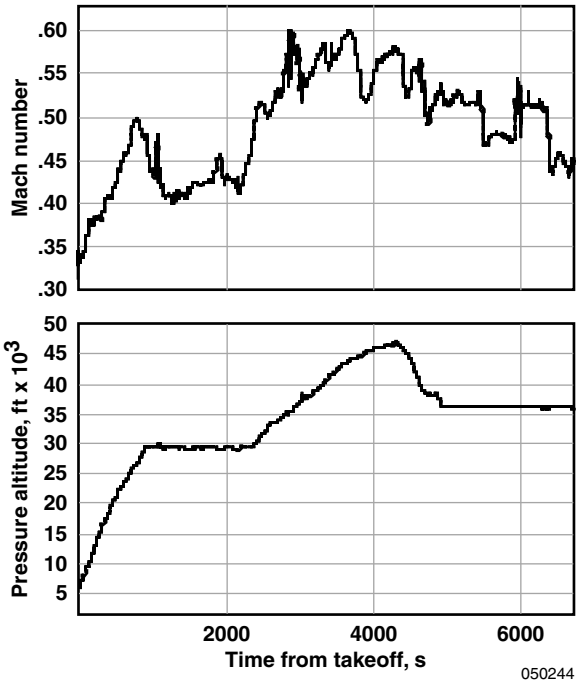

Figure 28. The X-38 Vehicle 132 captive-carry flight 2, Mach number and altitude profiles.

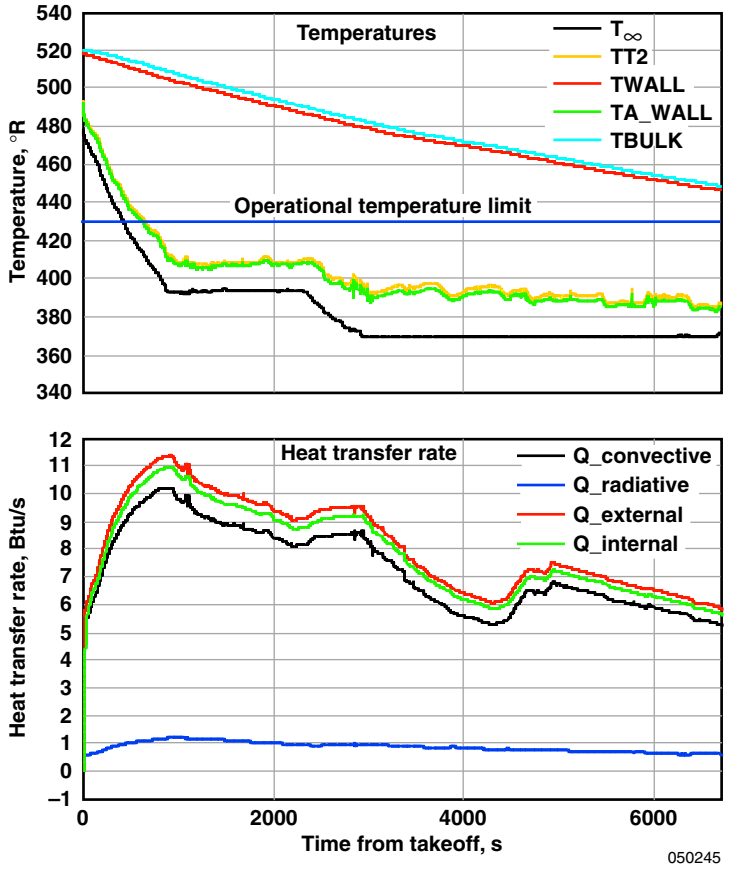

Figure 29. Results of cold-soak analysis starting from 80 degrees Fahrenheit.

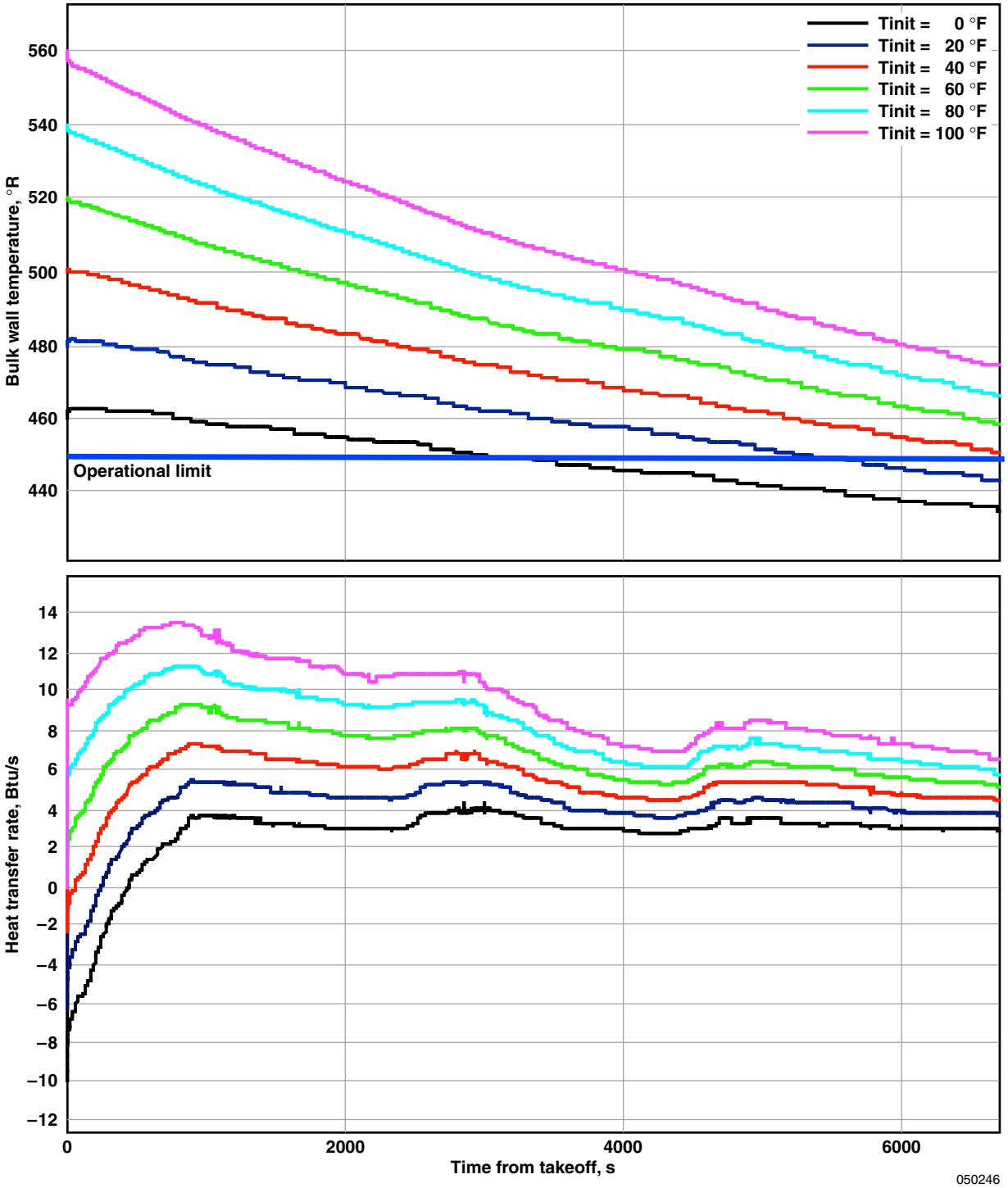

Figure 30. Effect of initial temperature on bulk temperature and heat transfer.

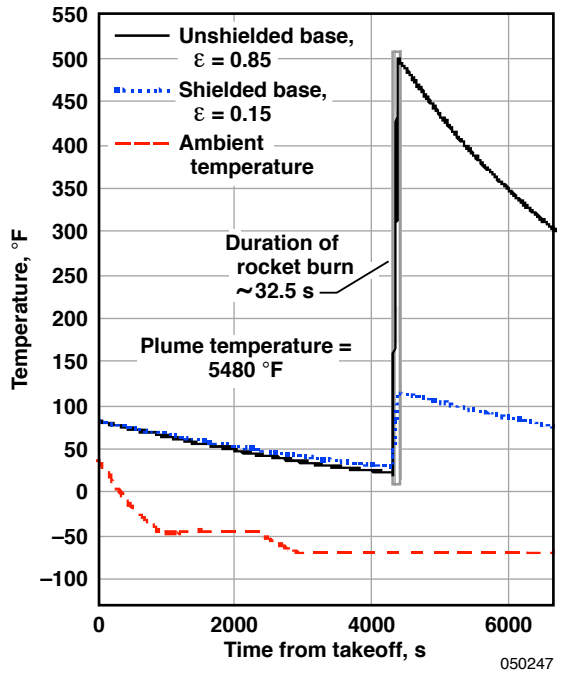

Figure 31. Time history of base temperatures with and without base shielding.

REPORT DOCUMENTATION PAGE

Form Approved
OMB No. 0704-0188

The public reporting burden for this collection of information is estimated to average 1 hour per response, including the time for reviewing instructions, searching existing data sources, gathering and maintaining the data needed, and completing and reviewing the collection of information. Send comments regarding this burden estimate or any other aspect of this collection of information, including suggestions for reducing this burden, to Department of Defense, Washington Headquarters Services, Directorate for Information Operations and Reports (0704-0188), 1215 Jefferson Davis Highway, Suite 1204, Arlington, VA 22202-4302. Respondents should be aware that notwithstanding any other provision of law, no person shall be subject to any penalty for failing to comply with a collection of information if it does not display a currently valid OMB control number.
PLEASE DO NOT RETURN YOUR FORM TO THE ABOVE ADDRESS.

1. REPORT DATE *(DD-MM-YYYY)*
01-03-2006

2. REPORT TYPE
Technical Publication

3. DATES COVERED *(From - To)*

4. TITLE AND SUBTITLE
Conceptual Design Study for an X-38 Transonic Rocket Assist Configuration

5a. CONTRACT NUMBER

5b. GRANT NUMBER

5c. PROGRAM ELEMENT NUMBER

6. AUTHOR(S)
Susan J. Stachowiak, Brent R. Cobleigh, Heather A. Maliska,
Masashi Mizukami, Stephen A. Whitmore, and Timothy H. Cox

5d. PROJECT NUMBER

5e. TASK NUMBER

5f. WORK UNIT NUMBER
953-50-00-SE-00-000

7. PERFORMING ORGANIZATION NAME(S) AND ADDRESS(ES)
NASA Dryden Flight Research Center
P.O. Box 273
Edwards, California 93523-0273

8. PERFORMING ORGANIZATION REPORT NUMBER
H-2583

9. SPONSORING/MONITORING AGENCY NAME(S) AND ADDRESS(ES)
National Aeronautics and Space Administration
Washington, DC 20546-0001

10. SPONSORING/MONITOR'S ACRONYM(S)
NASA

11. SPONSORING/MONITORING REPORT NUMBER
NASA/TP-2006-213672

12. DISTRIBUTION/AVAILABILITY STATEMENT
Unclassified -- Unlimited
Subject Category -- 05 Availability: NASA CASI (301) 621-0390 Distribution: Standard

13. SUPPLEMENTARY NOTES
An electronic version can be found at the NASA Dryden Flight Research Center Web site, under Technical Reports.

14. ABSTRACT
The X-38 Transonic Rocket Assist feasibility and conceptual design study examined the possibility of obtaining transonic flight data for the X-38 program by boosting an existing X-38 airframe into the transonic flight regime. The objective of the study was to develop a conceptual design to collect X-38 transonic aerodynamic flight data. This report summarizes the work performed by the conceptual design team in developing a proposed XTRA configuration. Initial study phases focused on selecting the appropriate vehicle to use for the transonic flight-test program, selecting the most appropriate propulsion system, and integrating the propulsion system with the X-38 vehicle. The final design featured two 10,000-lb thrust rocket motors, externally mounted on the sides of an X-38 flight-test vehicle. A detailed structural loads analysis of this configuration was performed and structure required for rocket attachment and jettison systems was designed. A ballast management system was developed to control changes in center of gravity caused by rocket burn and jettison. Simulation studies were performed to optimize the XTRA trajectory for maximum data collection potential and to identify any vehicle controllability issues. Simulation studies with this configuration show the potential for obtaining flight-test data at Mach numbers of up to 1.5.

15. SUBJECT TERMS
Atmospheric flight test, Rocket assist, Transonic aerodynamics, XTRA, X-15

16. SECURITY CLASSIFICATION OF:			17. LIMITATION OF ABSTRACT	18. NUMBER OF PAGES	19a. NAME OF RESPONSIBLE PERSON
a. REPORT	b. ABSTRACT	c. THIS PAGE			19b. TELEPHONE NUMBER *(Include area code)*
U	U	U	U	55	